

Introduction to SENG+ and its capabilities (Work Package: 4)

Vishnu Mohan¹, Nilanjan Chakraborty¹, R. Stewart Cant²
(Vishnu.Mohan@ncl.ac.uk)

¹School of Engineering, Newcastle University, Claremont Road, Newcastle-Upon-Tyne, NE1 7RU, UK

² Cambridge University Engineering Department, Trumpington Street, CB2 1PZ, UK

1st workshop of the ExCALIBUR Turbulence at the Exascale project (EP/W026686/1)

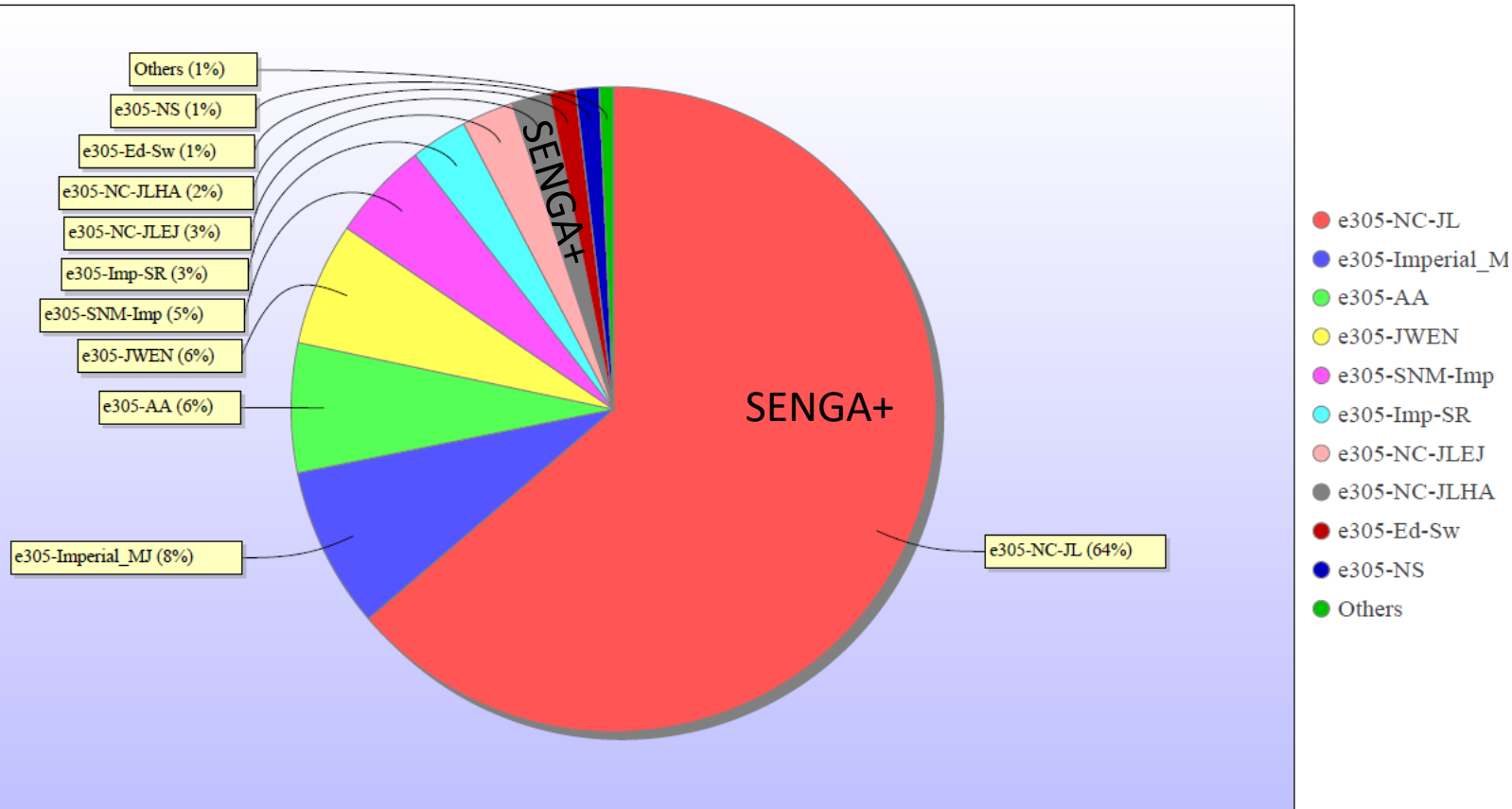
Imperial College London
29th September 2022



UNIVERSITY OF
CAMBRIDGE

SENGA+ as the UK community code

Computational time used by UKCTRF groups (Aug 2022):



- SENGAs/SENGA2 originally developed by Prof. R.S. Cant at Cambridge
- New functionalities (e.g. ignition modelling, multiphase, new boundary condition, flame-shock interaction, complex configuration, conjugate heat transfer) added by Prof. N. Chakraborty at Newcastle
- 66% of the UKCTRF computational time in the last allocation cycle was used by SENGAs users

International users of SENG+

UK

- Cambridge University
- Cranfield University
- Liverpool John Moores
- Newcastle University
- Daresbury Laboratory

Europe

- Universität der Bundeswehr München
- University of Eindhoven

North America

- Ontario Technical University

Asia

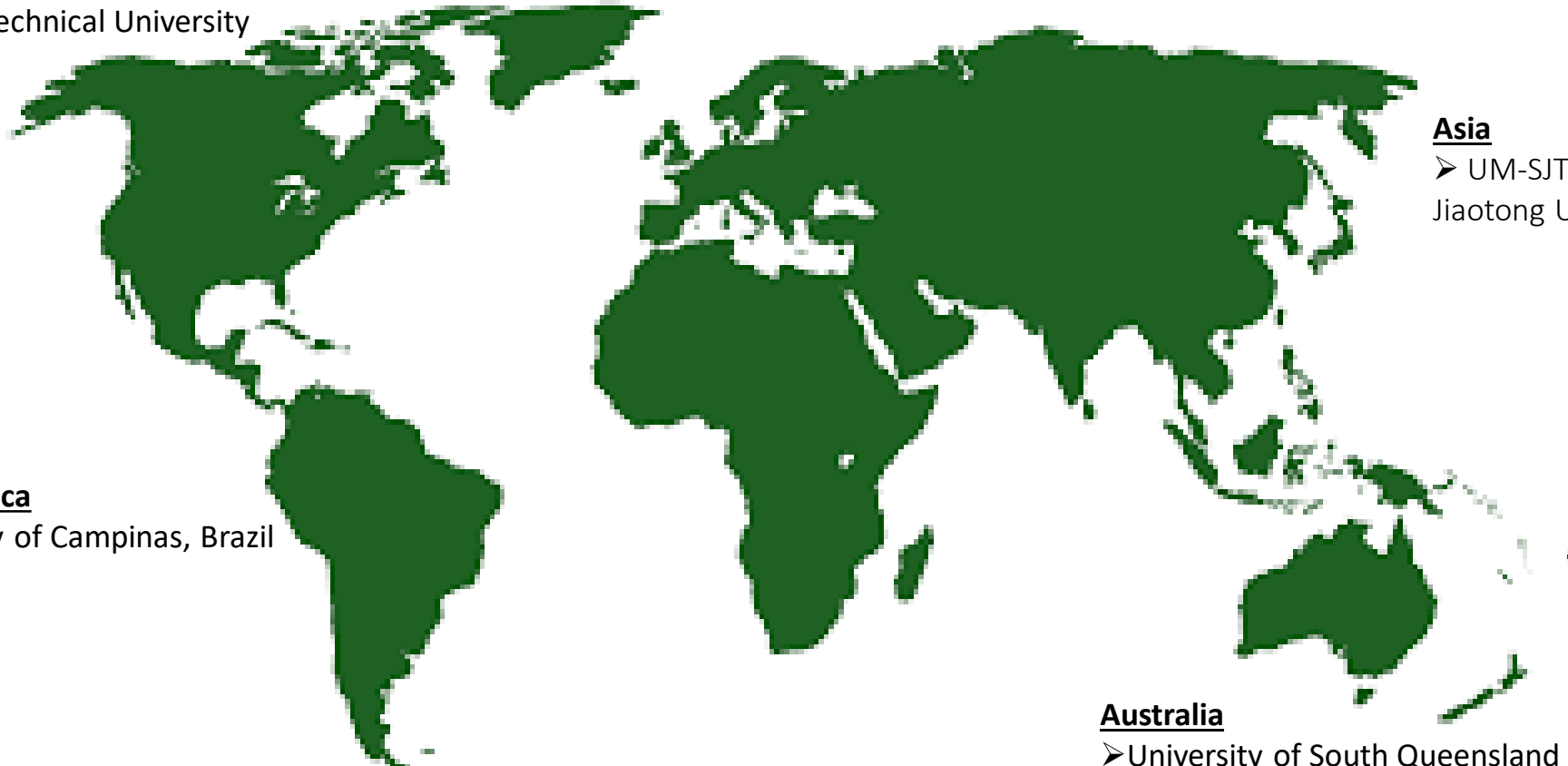
- UM-SJTU joint institute, Shanghai Jiaotong University

South America

- University of Campinas, Brazil

Australia

- University of South Queensland

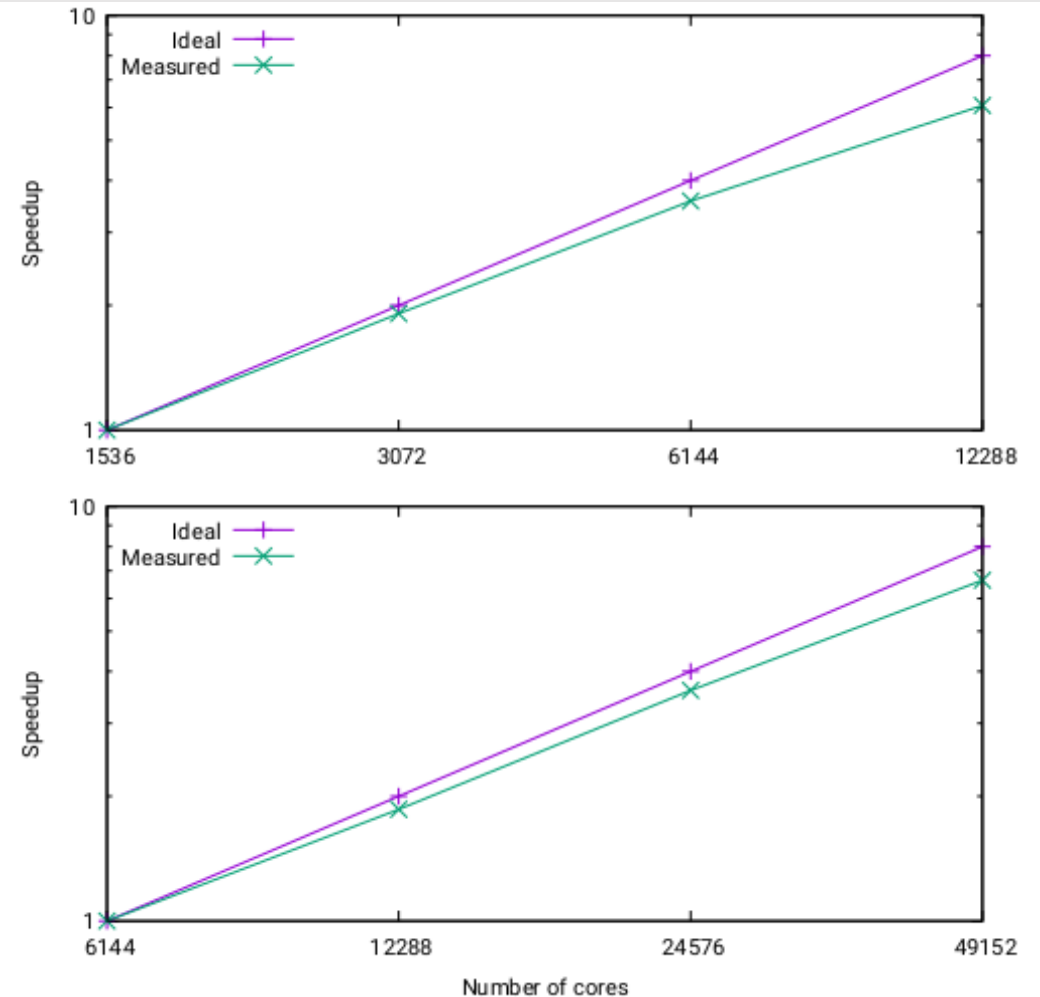
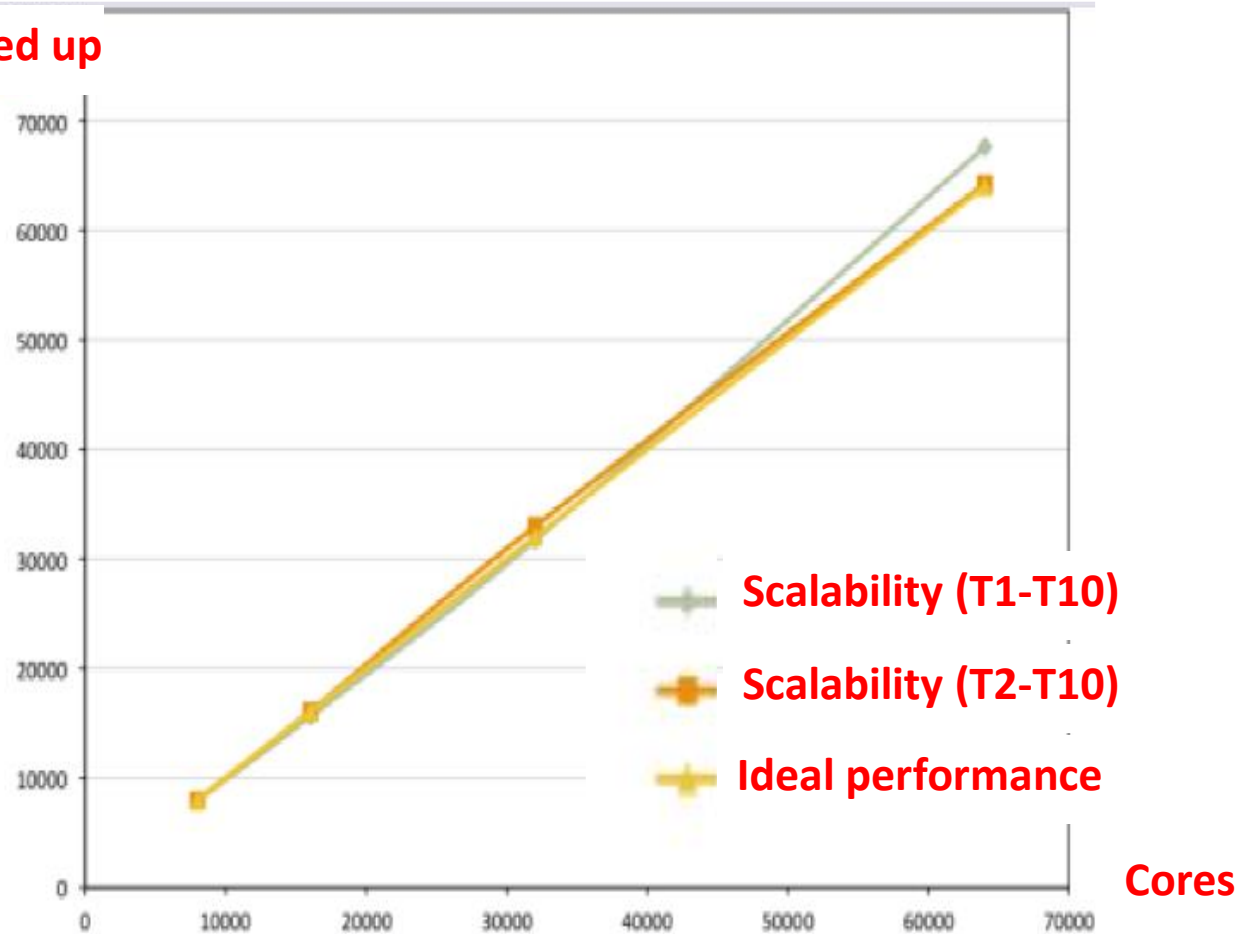


An introduction to SENGGA+

- SENGGA+ is a high-fidelity turbulent reacting flow solver, principally used for **Direct Numerical Simulations (DNS)** of turbulent reacting flows.
- Flagship code of the UK Consortium on Turbulent Reacting Flows (UKCTRF: www.ukctrf.com)
- Solves the governing equations of mass, momentum, energy and species for compressible turbulent reacting flows in 3D using a high-order finite-difference framework. Time stepping uses an **explicit RK method** with optional **implicit operator-splitting method for stiff chemical mechanisms**.
- Capable of simulating **single-phase** or **multi-phase** (e.g. droplet-laden or particle-laden) combustion processes. The dispersed phase is accounted for by Lagrangian tracking.
- Parallelised using **Message Passing Interface (MPI)**. Recent implementation of **HDF5 i/o**.
- Chemical reaction mechanism and molecular transport scheme can be chosen depending on the need.

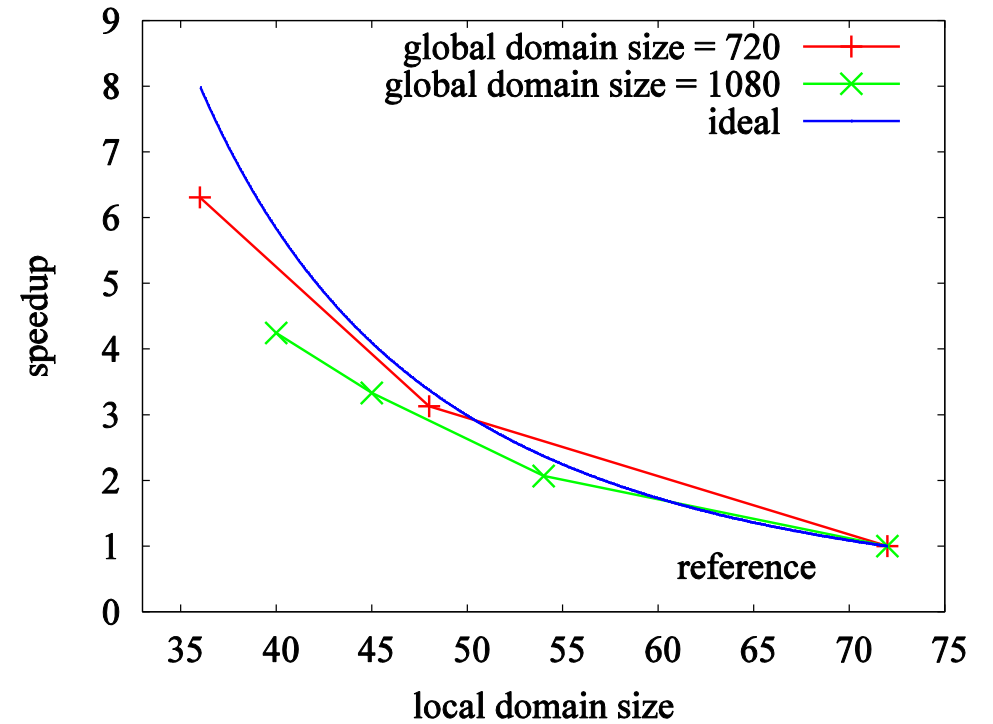
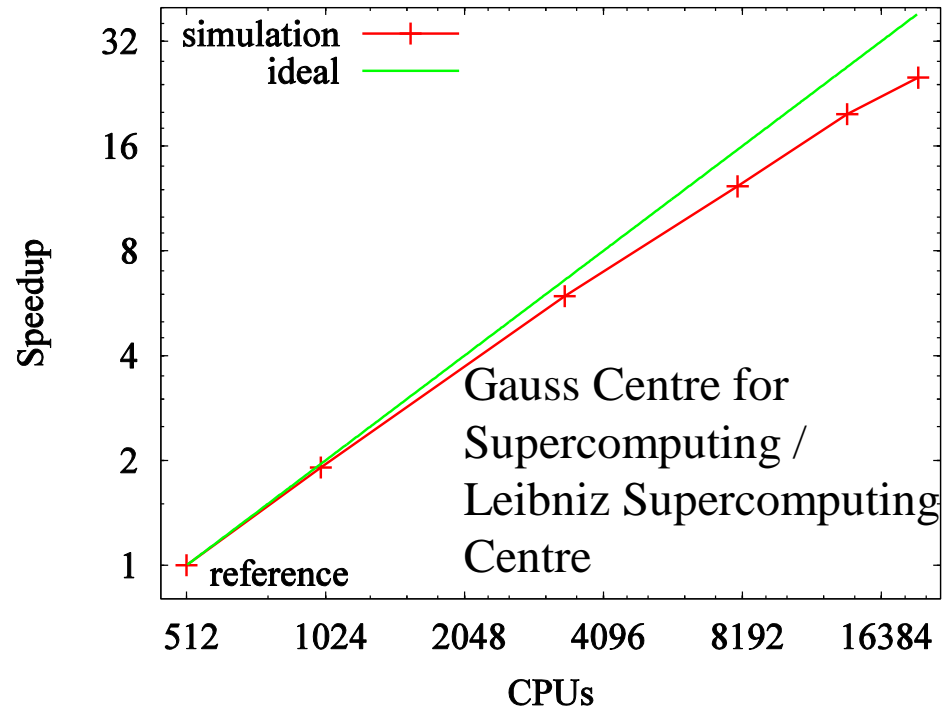
Parallel performance of SENGGA+ on ARCHER/2

Speed up



- Scaling exercise was conducted (at Daresbury, Dr J Grasset) using a premixed methane-air flame simulation involving 16 chemical species and 25 reactions

Parallel performance of SENGGA+ on international m/c



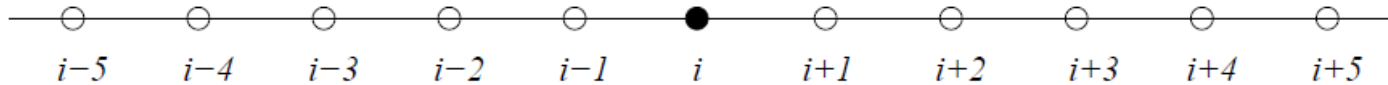
Left: Measured vs. ideal speedup on a domain consisting of 1080^3 mesh points.

Right: speedup relative to the local domain size for a global uniform 720^3 mesh and a global 1080^3 mesh

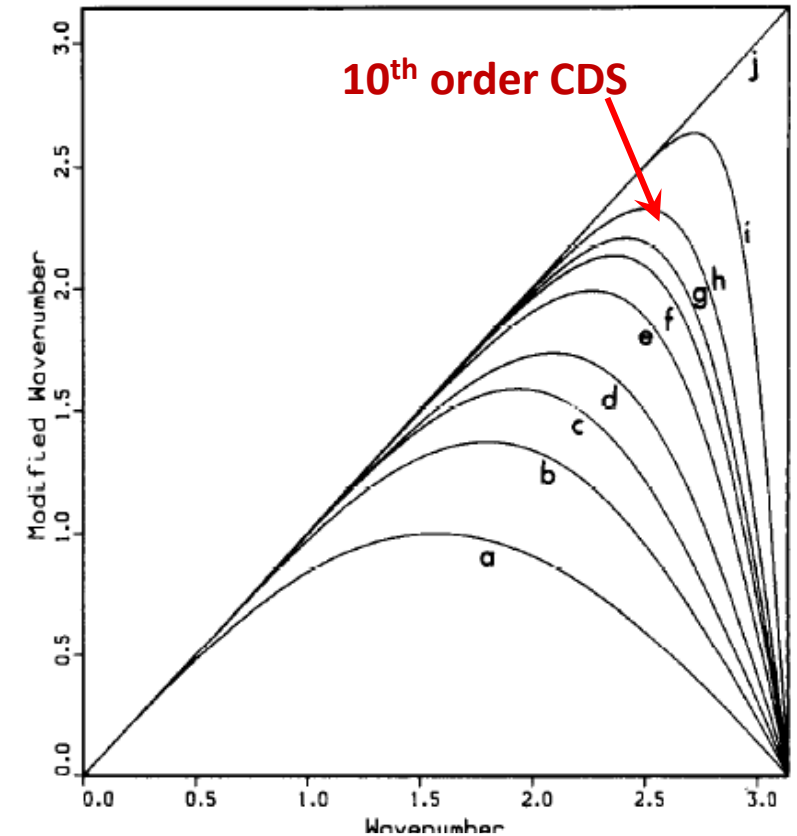
Spatial discretisation in SENGGA+

- Spatial discretisation uses a 10th order central difference scheme for the internal grid points. The order of accuracy drops gradually to a 4th order one-sided scheme at the non-periodic boundaries.

- 10th order central difference scheme provides accuracy comparable to a spectral scheme, but with greater flexibility and ease of parallelisation.



- Scheme requires a stencil of 11 points. This implies a halo of 5 points around each parallel subdomain.




Time advancement in SENGGA+

- Explicit time advancement uses a low storage (two registers) 3rd /4th order explicit Runge-Kutta scheme.

$$\frac{\partial \mathbf{U}}{\partial t} = \mathbf{R}(\mathbf{U}, t) \quad \text{For s-stage Runge-Kutta scheme}$$

$\mathbf{U} = \{\rho, \rho u, \rho v, \rho w, \rho E, \rho Y_\alpha\}^T$


$$\begin{aligned} \mathbf{U}^{(i)} &= \mathbf{U}^{(n)} + \delta t \sum_{j=1}^{i-1} a_{ij} \mathbf{R}^{(j)} \\ \mathbf{U}^{(n+1)} &= \mathbf{U}^{(n)} + \delta t \sum_{j=1}^s b_j \mathbf{R}^{(j)} \\ t^{(i)} &= t^{(n)} + c_i \delta t \\ \hat{\mathbf{U}}^{(n+1)} &= \mathbf{U}^{(n)} + \delta t \sum_{j=1}^s \hat{b}_j \mathbf{R}^{(j)} \end{aligned}$$

- Adaptive time step size estimated using a PID-type controller.
- For stiff chemistry, the equations are time-advanced using an a semi-implicit additive Runge-Kutta method where a linear system of ODEs is solved using preconditioned Krylov iteration as implemented in the VODPK package.

Multi-phase flow (1)

Liquid (Dispersed) Phase:

Lagrangian Approach is used for sub-grid spherical droplets following the approach:

- Position: $\frac{d\vec{x}_d}{dt} = \vec{u}_d$
- Velocity: $\frac{d\vec{u}_d}{dt} = \frac{\vec{u}(\vec{x}_d, t) - \vec{u}_d}{\tau_d^u}$
- Diameter: $\frac{da_d^2}{dt} = \frac{a_d^2}{\tau_d^p}$
- Temperature: $\frac{dT_d}{dt} = \frac{\hat{T}(\vec{x}_d, t) - T_d - B_d L_v / C_p^g}{\tau_d^T}$

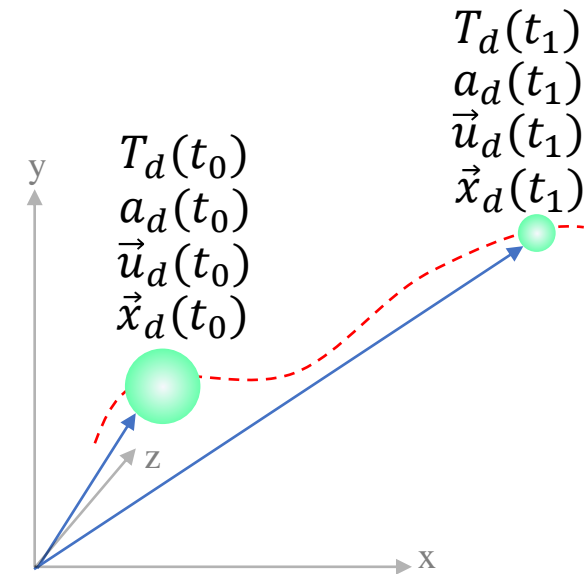
L_v is the latent heat of vaporization

B_d is the Spalding mass transfer number

C_p^g is the gaseous specific heats at constant pressure

Relaxation time scales associated with droplet:

- Velocity, τ_d^u
- Diameter, τ_d^p
- Temperature, τ_d^T



Multi-phase flow (2)

Gaseous Phase:

Eulerian Approach is used to solve for gas phase combustion.

Coupling between two phases:

$$\frac{\partial \rho \psi}{\partial t} + \frac{\partial \rho u_j \psi}{\partial x_j} = \frac{\partial}{\partial x_j} \left(\Gamma_\psi \frac{\partial \psi}{\partial x_j} \right) + \dot{w}_\psi + \dot{S}_g + \dot{S}_\psi$$

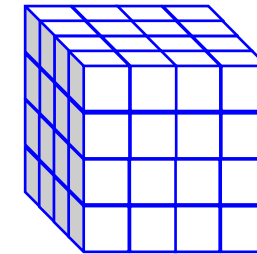
$\psi_1 = \{1, u_i, \hat{T}, Y_F, Y_O\}$ for $\psi = \{1, u_j, e, Y_F, Y_O\}$

$\Gamma_\psi = \rho \nu / \sigma_\psi$ for $\psi = \{1, u_i, Y_F, Y_O\}$ and $\Gamma_\psi = \lambda$ for $\psi = e$

\dot{w}_ψ is chemical reaction rate,

\dot{S}_g is an appropriate source/sink term and

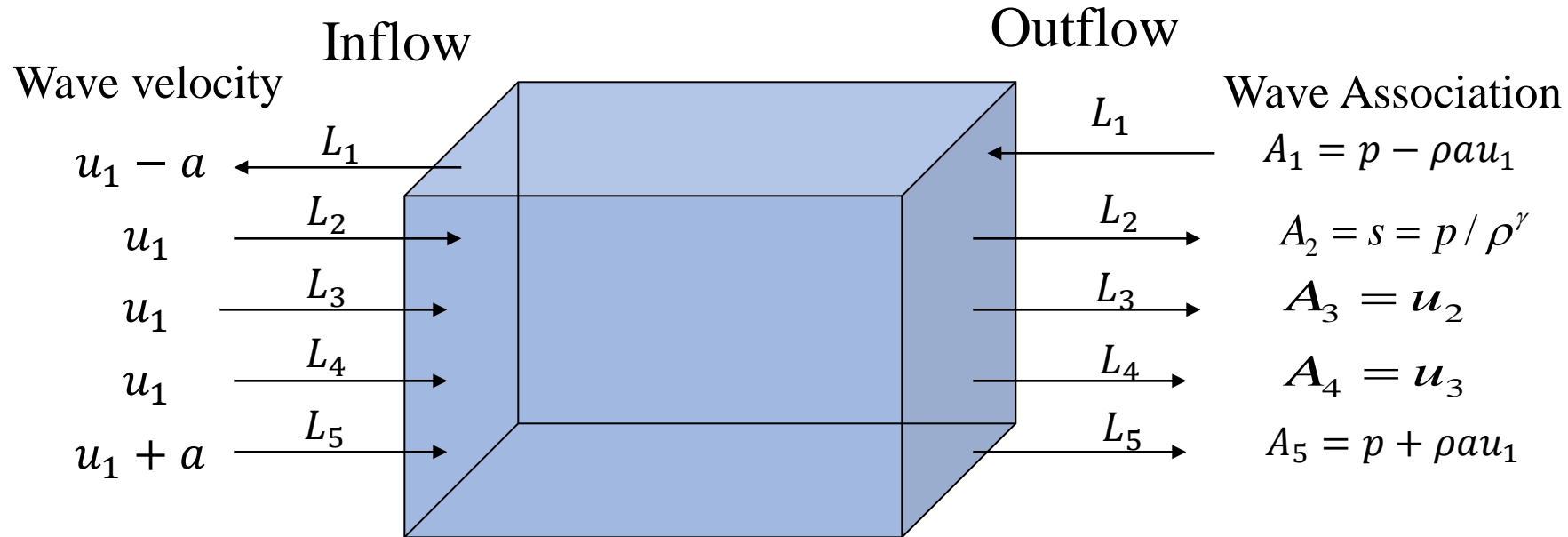
\dot{S}_ψ is *source term due to droplet evaporation*, which is tri-linearly interpolated from the droplet's sub-grid position, \vec{x}_d , to the eight surrounding nodes.



$\vec{u}(x, y, z, t)$
 $e(x, y, z, t)$
 $Y_F(x, y, z, t)$
 $Y_O(x, y, z, t)$

Ideal gas law is considered for gaseous reacting mixtures

Boundary conditions in SENGGA+



Wave amplitude variations into and out of the inflow and outflow boundary

For non-reflecting boundary incoming $L_i = 0$

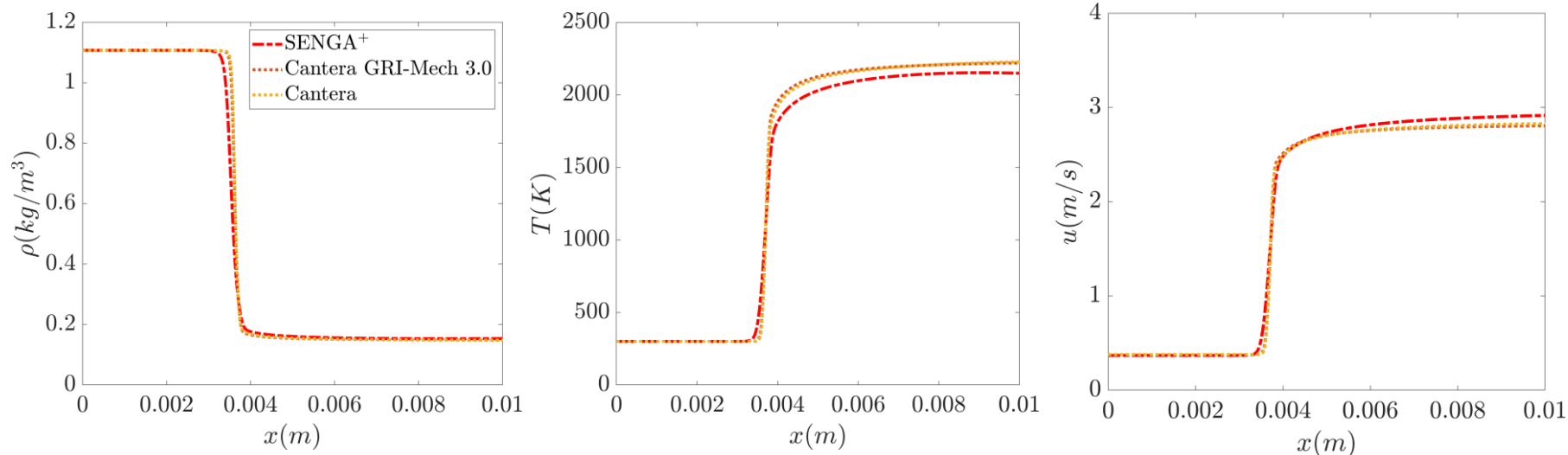
For partially non-reflecting boundary incoming $L_i = K (p - p_{req})$

Boundary conditions in SENGGA+

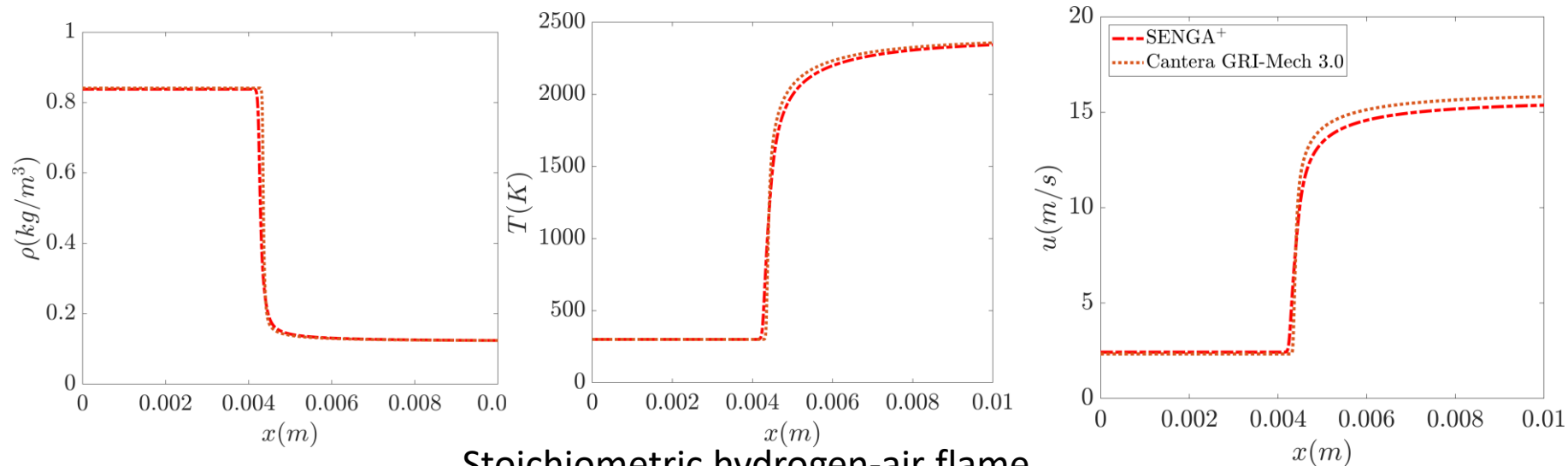
- ❑ Boundary conditions specified using the Navier Stokes Characteristics Boundary Conditions (NSCBC) formulation by Poinso & Lele (1992)
- ❑ Incoming wave amplitude variations are specified from BC information
- ❑ Outgoing wave amplitude variations are evaluated from internal information

- ❑ SENGGA+ has BCs for partially non-reflecting outflow, reflecting or non-reflecting inflow, isothermal or adiabatic walls and periodic boundaries.
- ❑ Ongoing work includes implementation of improved NSCBC boundary conditions, conjugate heat transfer and immersed boundary methods.

Validation of SENGAs: Chemistry

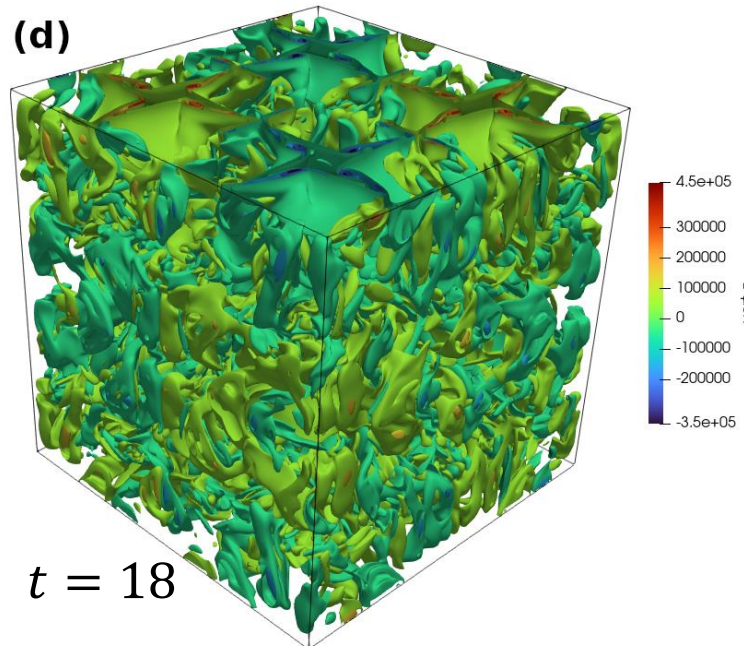
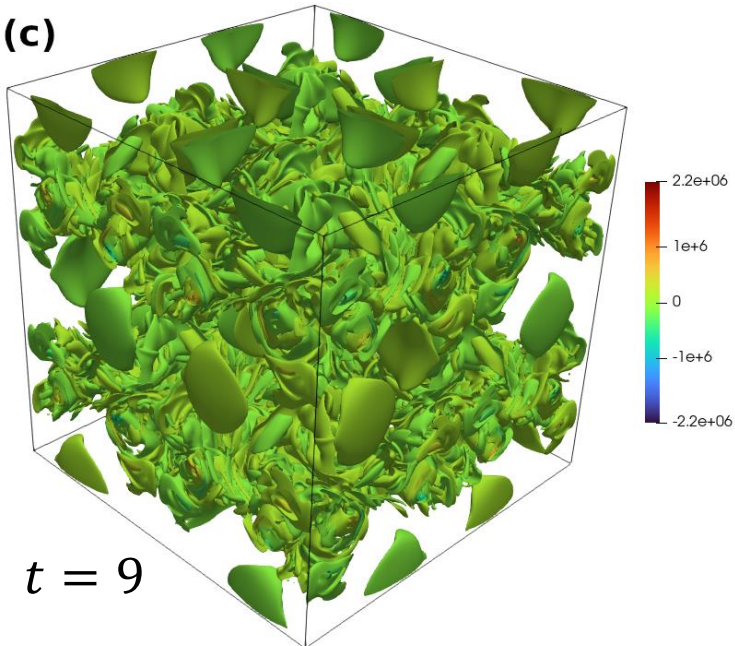
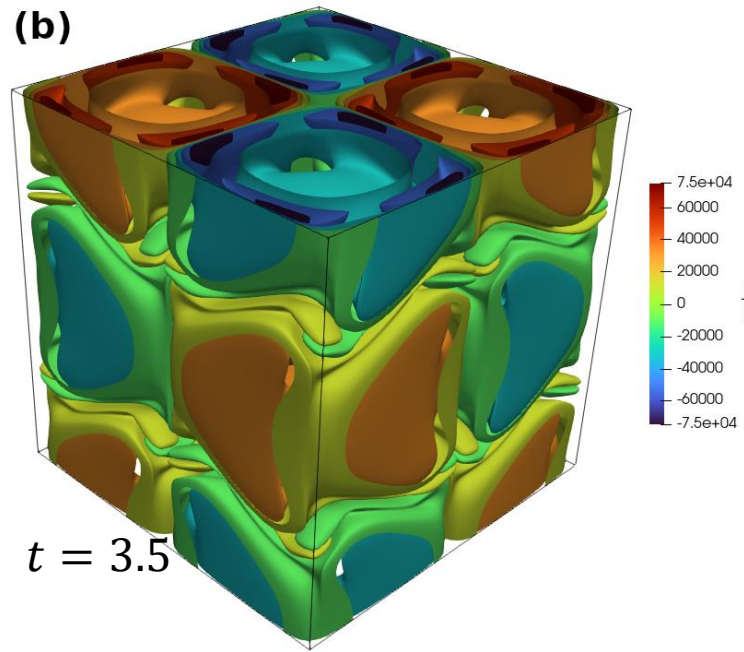
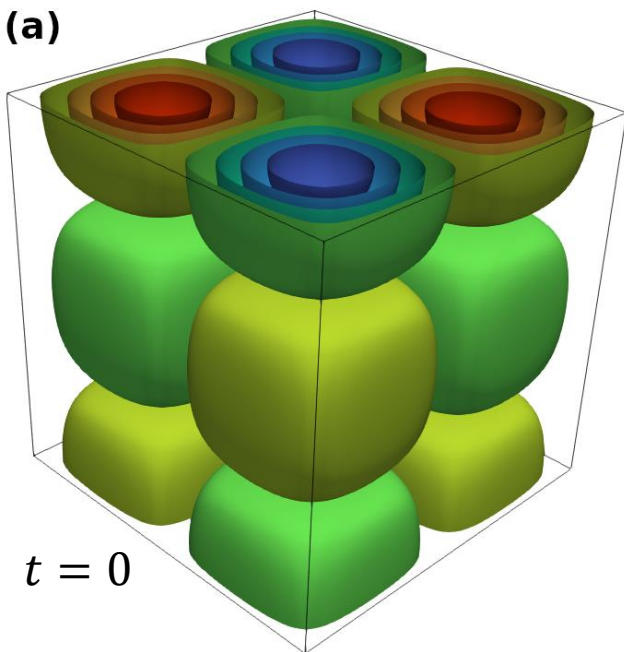


Stoichiometric methane-air flame



Stoichiometric hydrogen-air flame

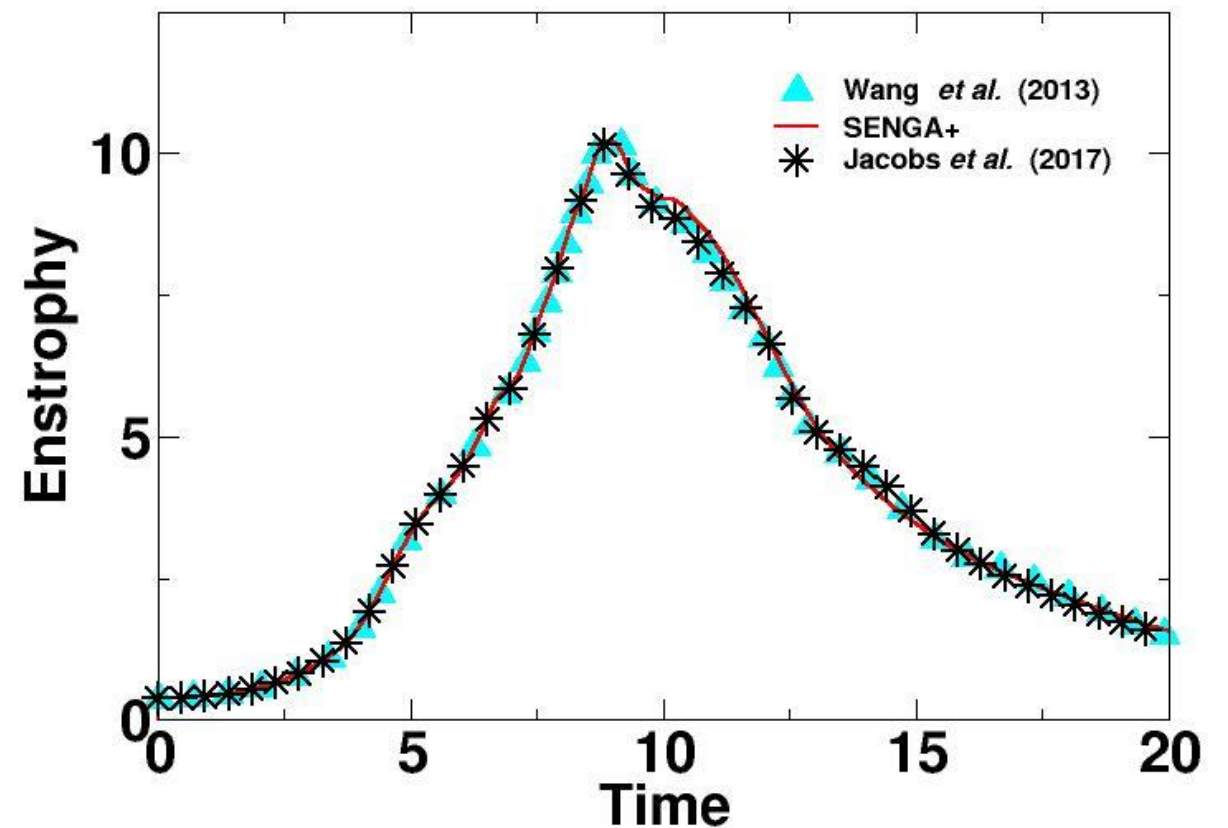
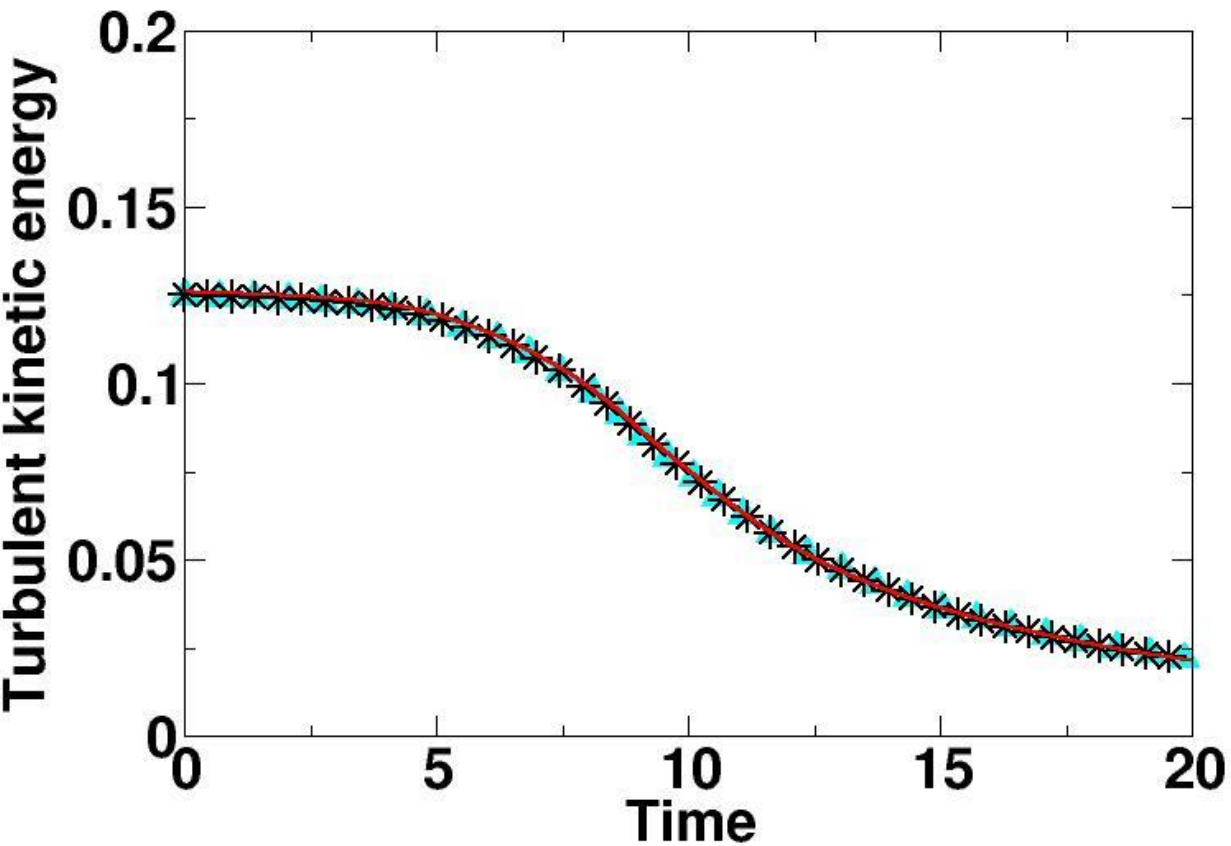
Validation of SENGGA+: Turbulence



Non-dimensionalised time $t = \frac{\hat{t}}{L/U_0}$

Z-vorticity contours

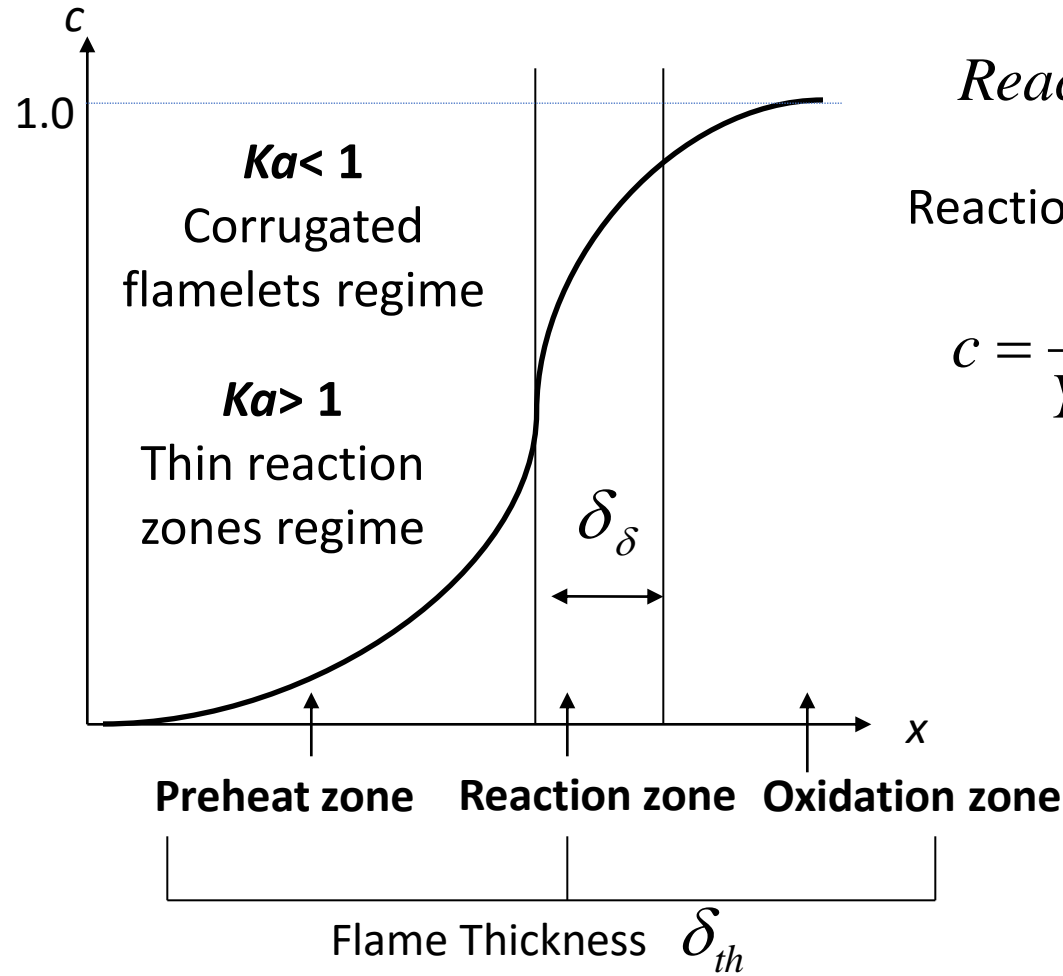
Validation of SENGAs: Turbulence



Taylor-Green vortex test case

Turbulent premixed combustion

Premixed Flame Structure



Reaction Mechanism :

Reactants \rightarrow Products

Reaction progress variable:

$$c = \frac{Y_P - Y_{P0}}{Y_{P\infty} - Y_{P0}}; \quad c = \frac{Y_{R0} - Y_R}{Y_{R0} - Y_{R\infty}}$$

Karlovitz number :

$$Ka = \frac{\delta_{th}^2}{\eta^2} = \frac{v_\eta^2}{S_L^2}$$

Damköhler number : $Da = \frac{l S_L}{u' \delta_{th}}$

Computational cost of Combustion DNS

Computational cost of DNS of non-reacting incompressible flows:

$$w \sim N_L^3 N_t \sim n_l^3 n_t \text{Re}_t^{11/4}$$

Computational cost of DNS of non-reacting compressible flows (for explicit time marching):

$$w \sim N_L^3 N_t \sim n_l^3 n_t \text{Re}_t^3 / \text{Ma}$$

Computational cost of DNS of compressible reacting flows:

$$w \sim N_L^3 N_t \sim n_l^3 n_t \text{Re}_t^3 / \text{Ma} * (Q^3 / Ka^{3/2})$$

n_l : Number of integral eddies within the domain

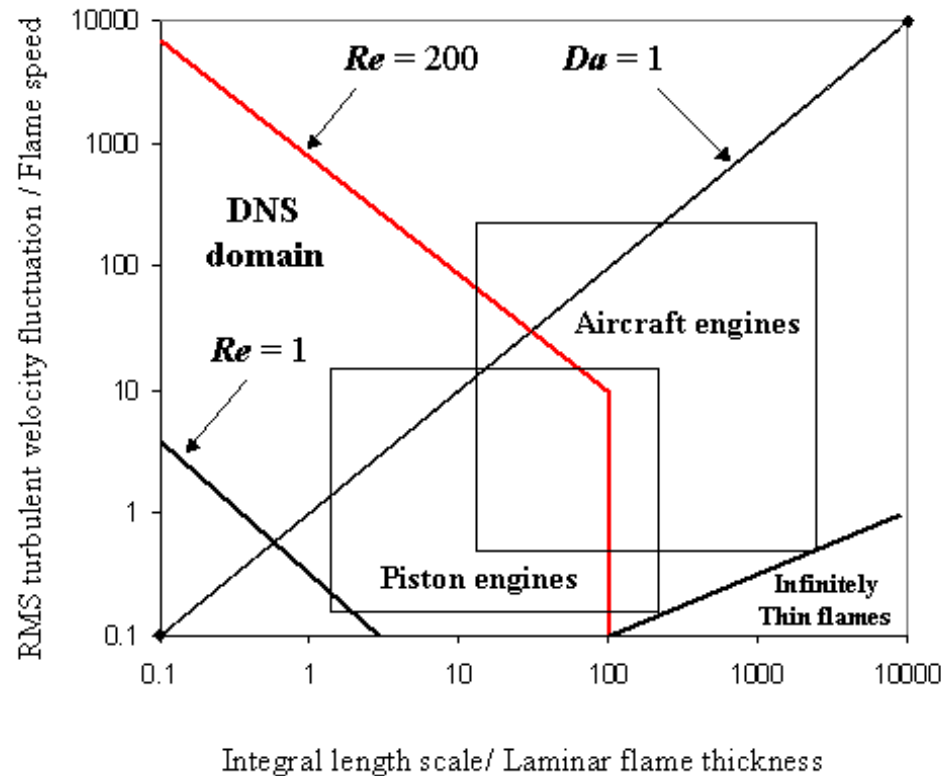
n_t : Number of integral eddy turn over times

Q : Number of grid points to resolve the flame thickness ($Q \sim 10-20$)

Ka : Karlovitz number ($Ka \sim \delta_{th}^2 / \eta^2$)

Computational cost of Combustion DNS

Chemistry is modelled in combustion DNS



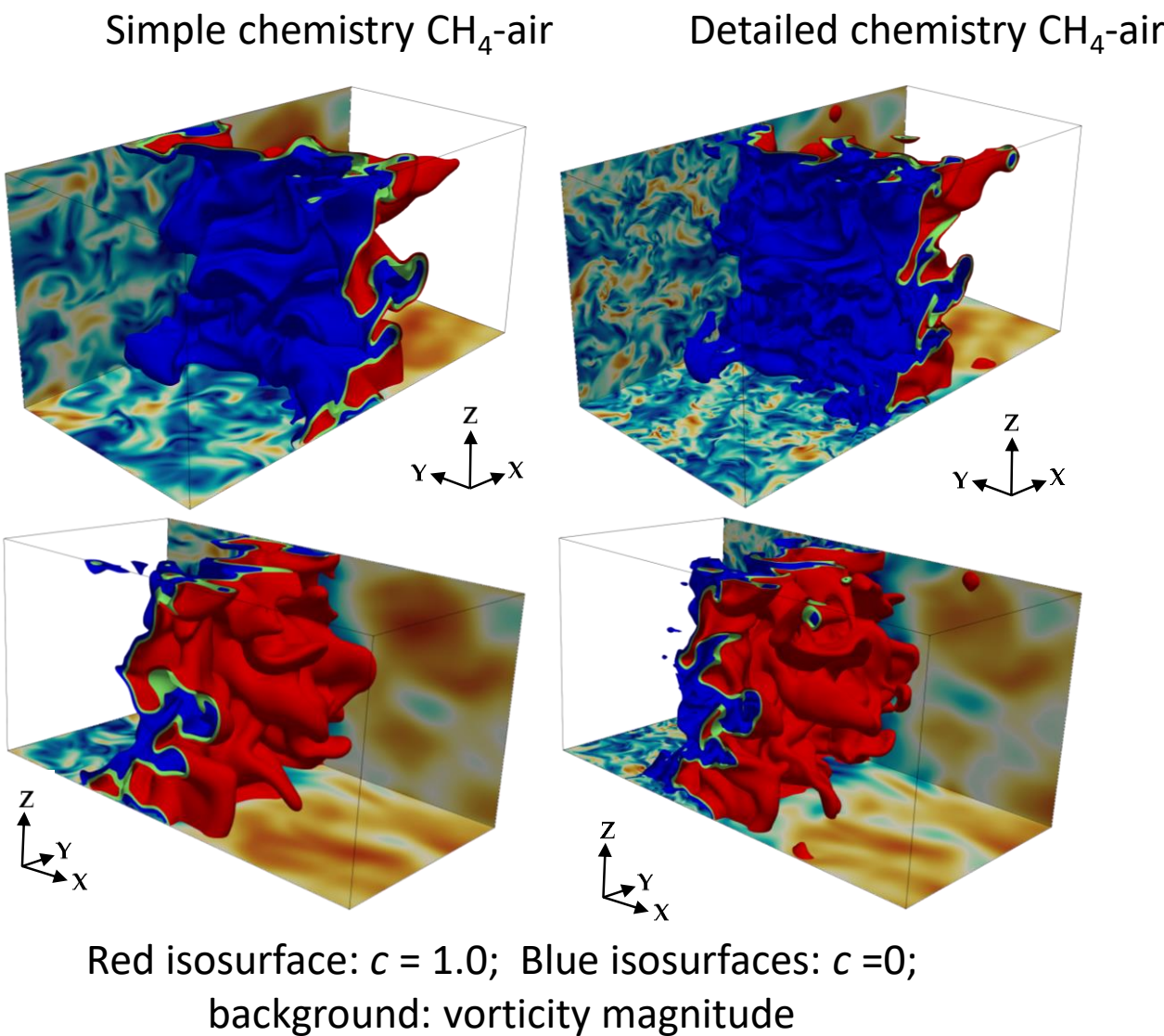
❑ A skeletal propane-air reaction mechanism involves 27 species and 73 reactions.

❑ Simulation of a flame would require 1000000 time steps.

❑ With present algorithms this would take 500 CPU years on a teraflop computer and 1000 terabytes of memory.

The full chemical mechanism of isooctane-air mixture requires more than 800 species and 3500 chemical reactions

Comparison between simple chemistry and detailed chemistry simulations

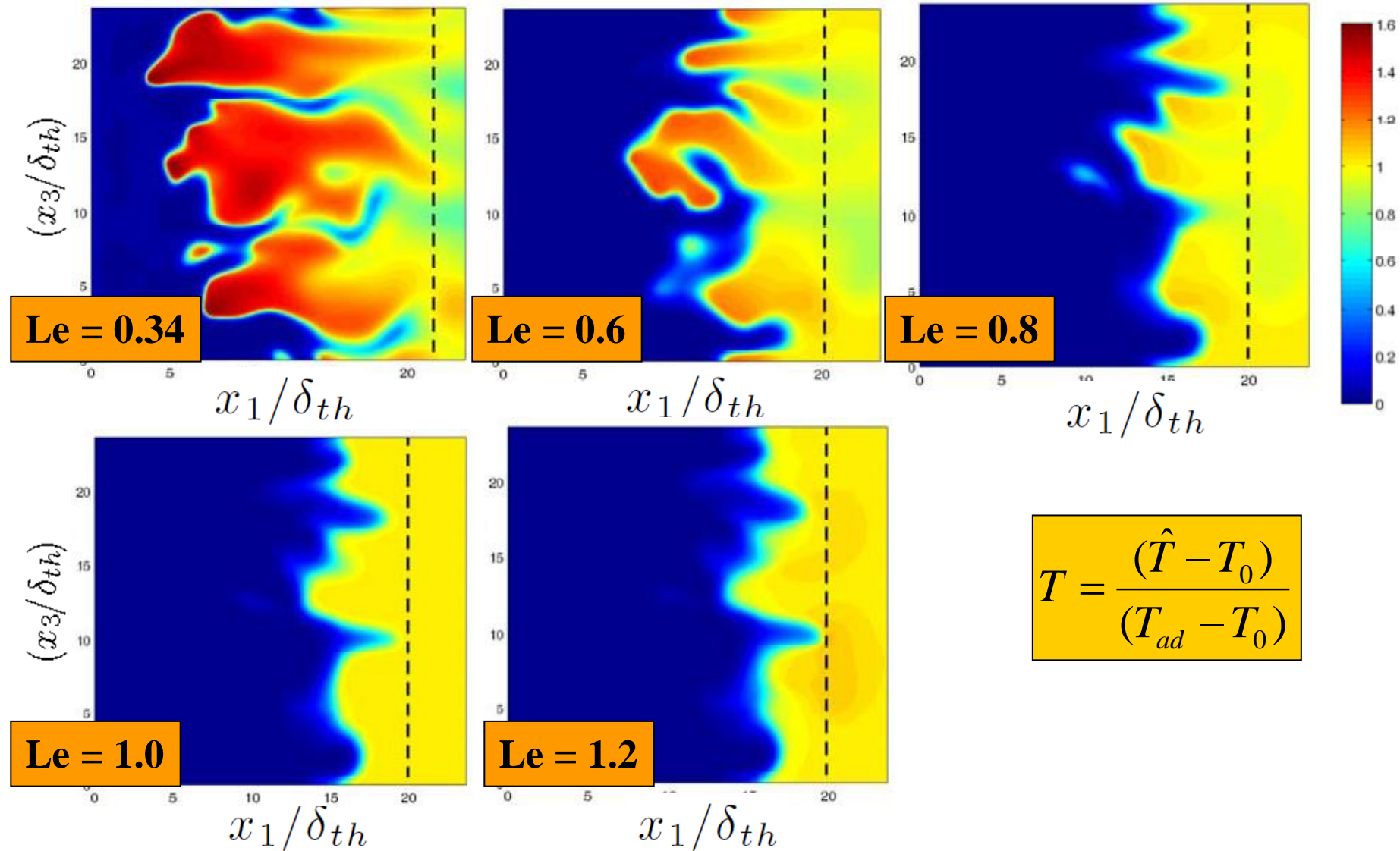


Method	Simple Chemistry and Transport	Detailed Chemistry and Transport
Estimated carbon footprint	$\sim 25\text{ kg CO}_2$	$\sim 10^3\text{ kg CO}_2$
CPU cost	$O(10^5)$ CPU hours [32,33]	$O(10^7)$ CPU hours [3]
Data volume	$O(1)$ TB [32,33]	$O(100)$ TB [3]
Parametric variations	Dozens possible [32,33]	Typically, very few (e.g 1-4) [34-37]; more limited in terms of nondimensional numbers, pressure or size of domain.
Data analysis	Straightforward, unambiguous results.	Complex (due to re-evaluation of constitutive laws); Results are not unambiguous due to different possibilities to define reaction progress variable (RPV) [34-36]

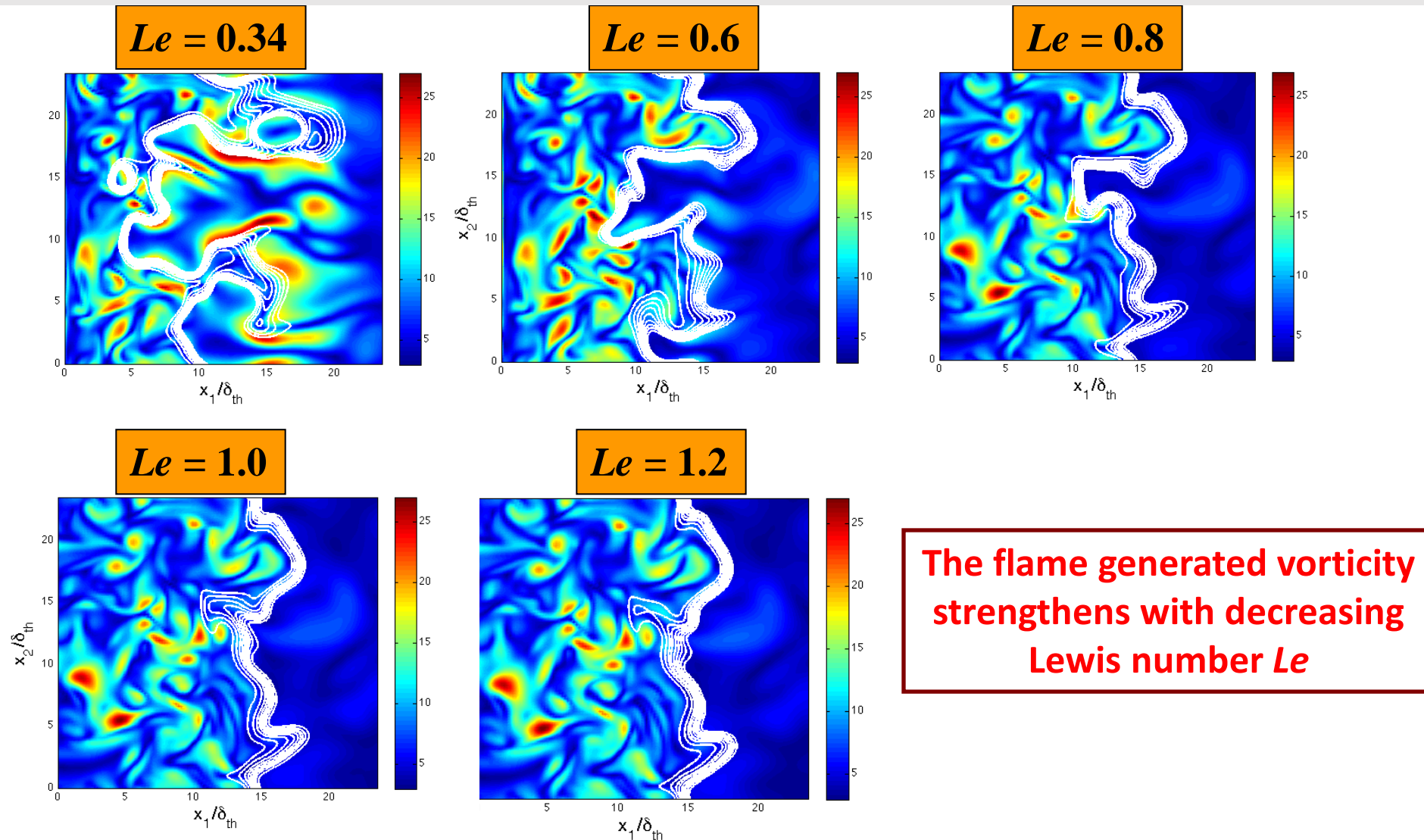
Implications of chemical representation

- For typical hydrocarbon and hydrogen flames the CPU cost, data volume and carbon footprint for detailed chemical mechanisms are often 10^2 times of that of the cost for the same problem with simple chemistry.
- It is difficult to carry out a large parametric variation with the detailed chemistry because of computational cost but parametric analysis is routinely done using simple chemistry. The cost saved by using a simple chemistry can be used to address turbulent reacting flow problems in relatively complex flow configurations.
- Data analysis for simple chemistry simulations is relatively simple and the comparison with analytical results is relatively straightforward. Key variables such as reaction progress variable cannot be defined uniquely for detailed chemistry.
- Problems where autoignition, preferential diffusion and flameless combustion play key roles cannot be addressed using simple chemistry. However, the standard flame propagation, flame-wall interaction and localised ignition statistics can be captured by simple chemistry.

Lewis number effects on non-dimensional temperature T field

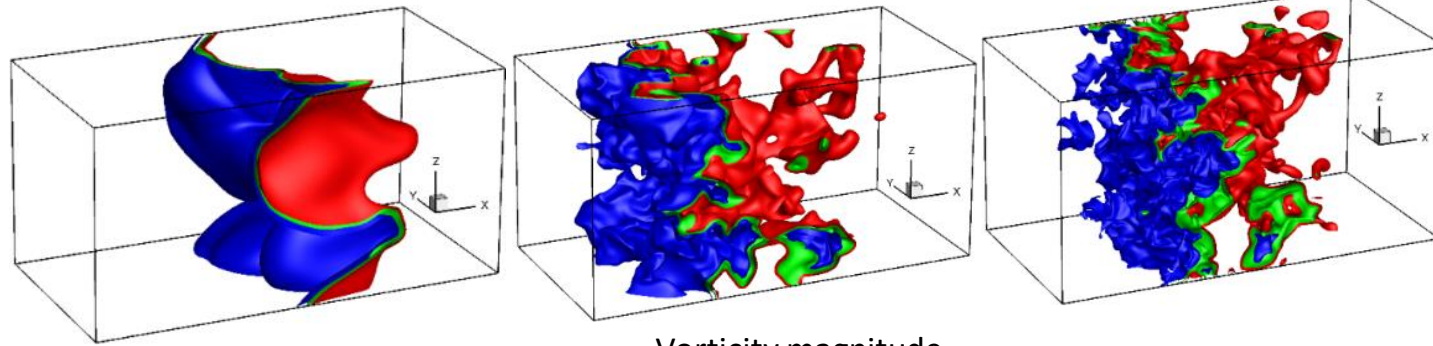
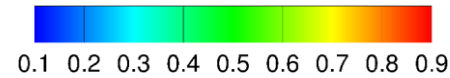


***Le* effects on distribution of vorticity $\sqrt{\omega_i \omega_i} \times \delta_{th} / S_L$**

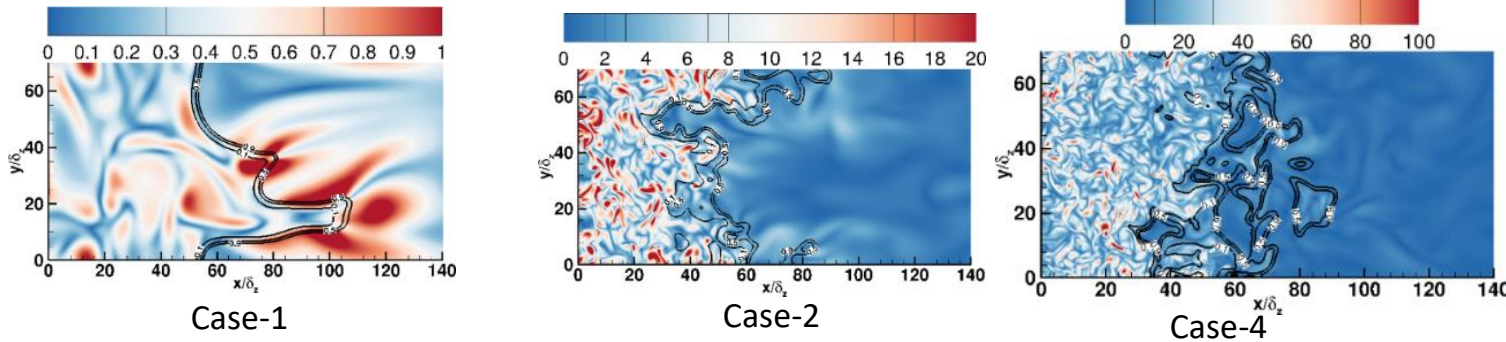


Flame area & volume-integrated burning rate for statistically planar flames

Progress variable

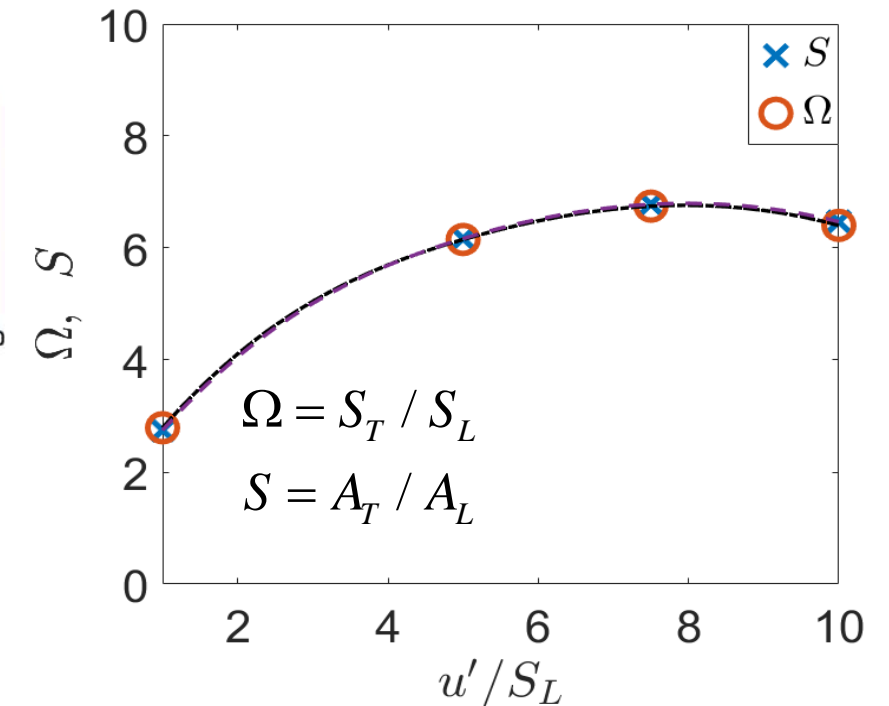


Vorticity magnitude

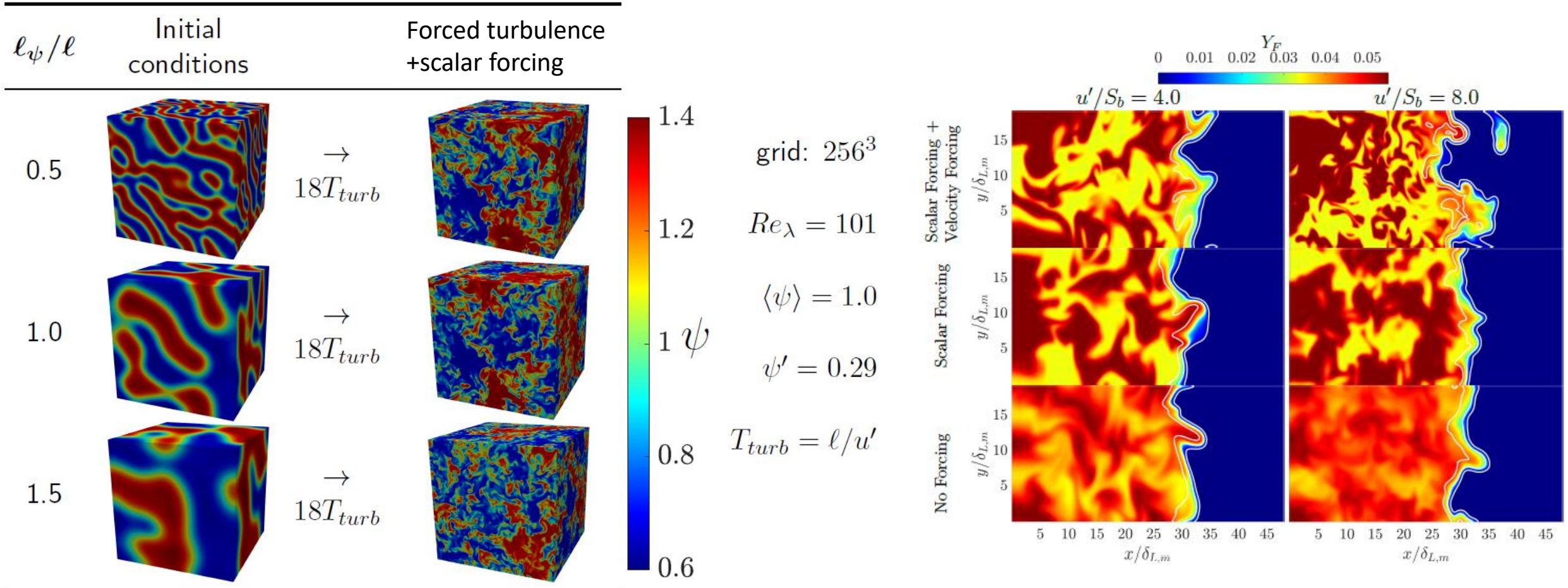


	u'/S_L	Ka	Da	Re_l
Case-1	1	0.577	3	7.56
Case-2	5	6.454	0.6	37.80
Case-3	7.5	11.858	0.4	56.70
Case-4	10	18.257	0.3	75.60

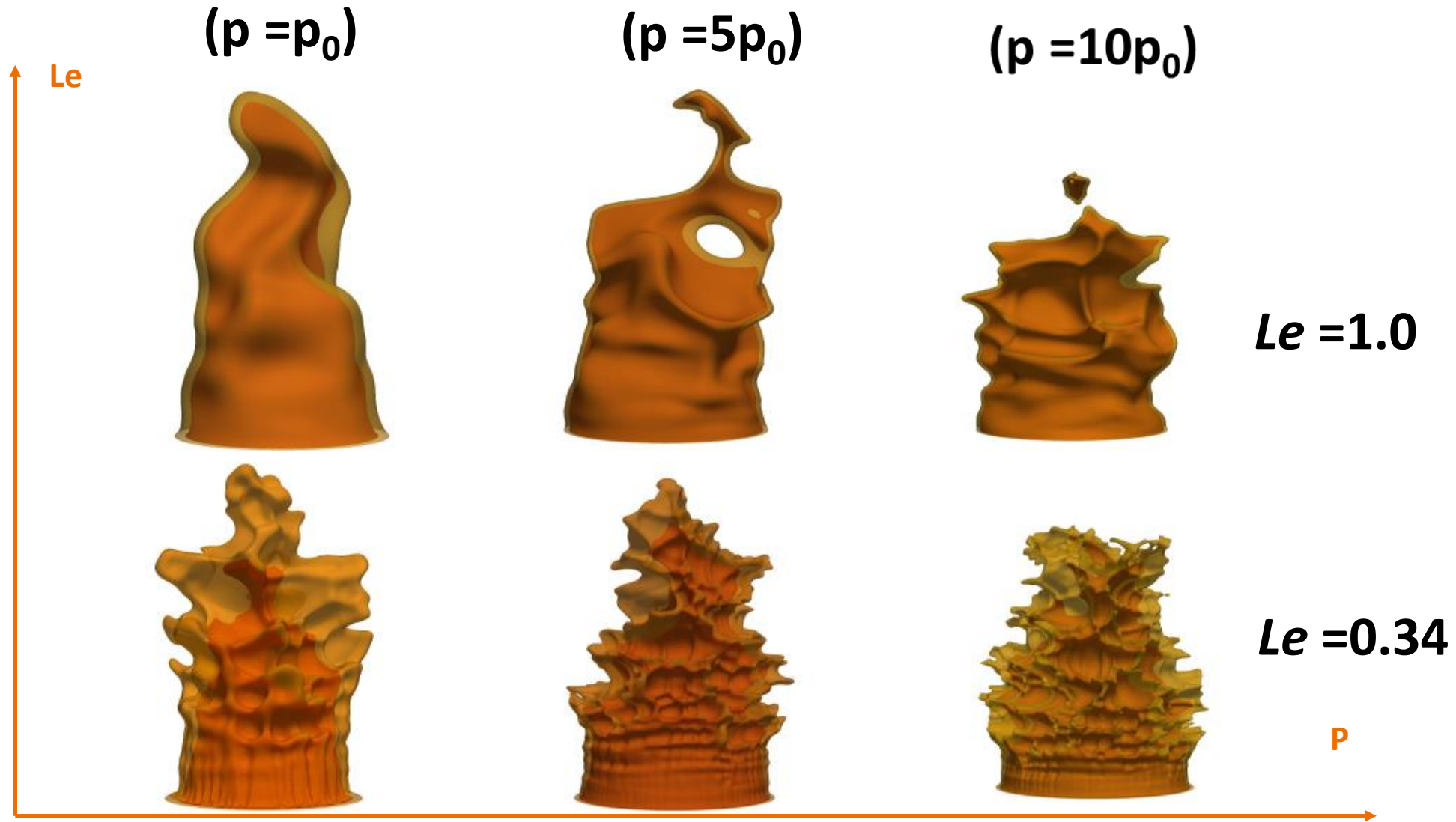
- Turbulent planar flame simulations have been performed.
- Turbulence is forced upstream of the flame using modified Lundgren's forcing.



Scalar forcing and stratified mixture combustion

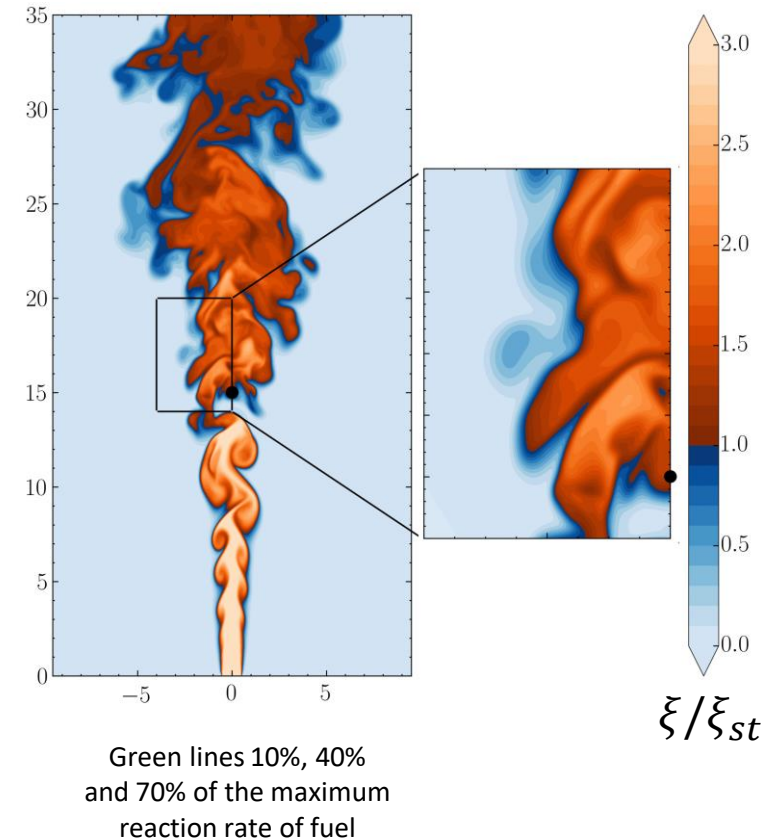
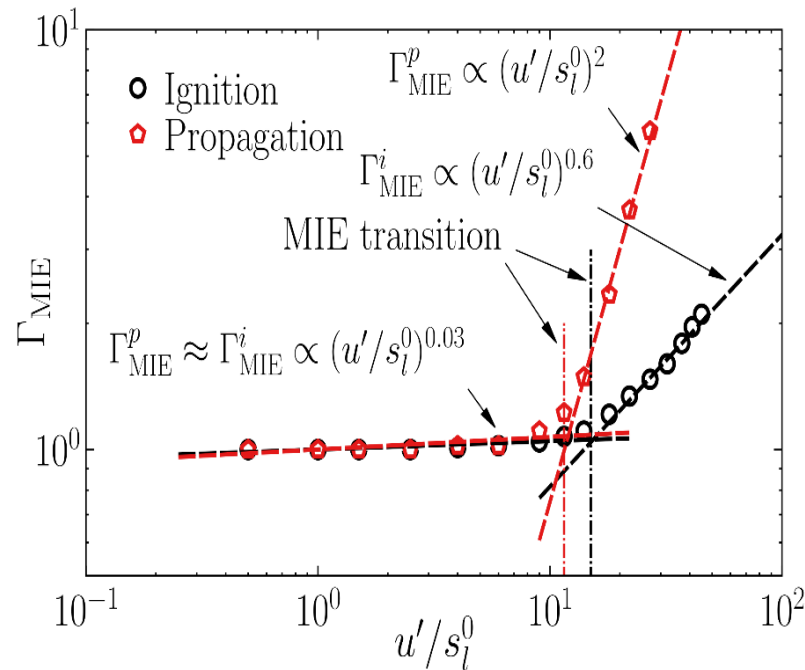
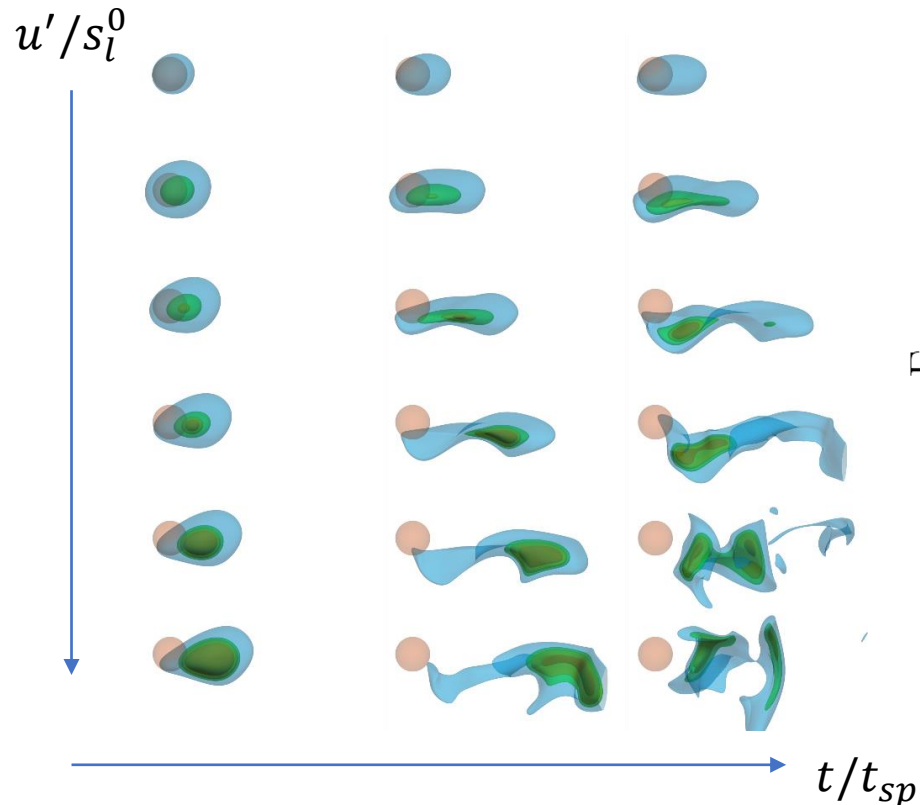


High-pressure turbulent premixed Bunsen flames

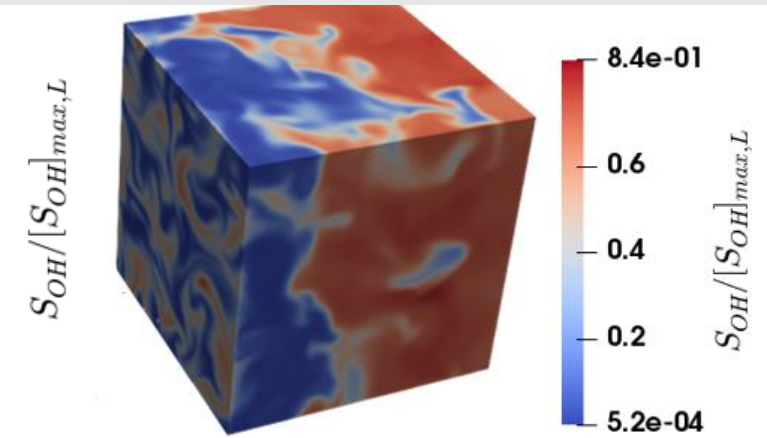
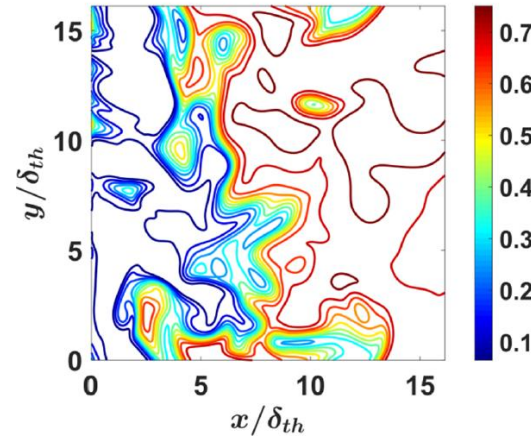


Localised forced ignition

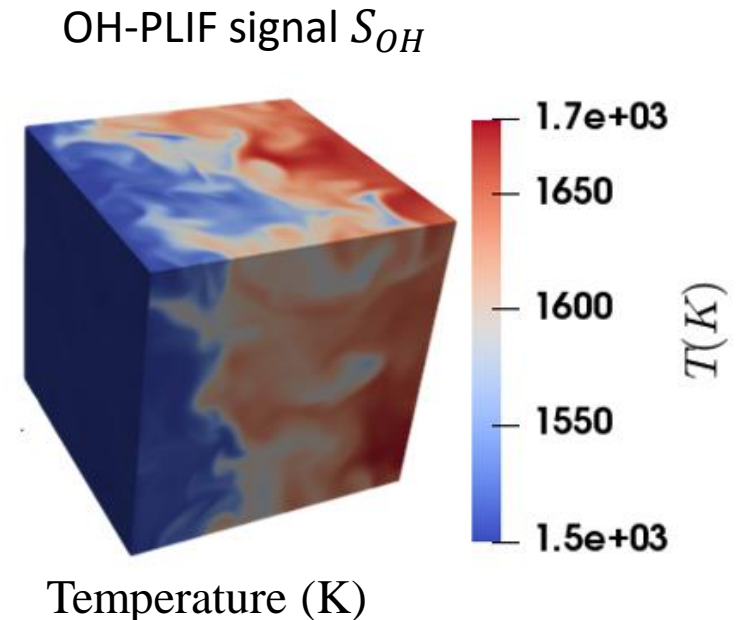
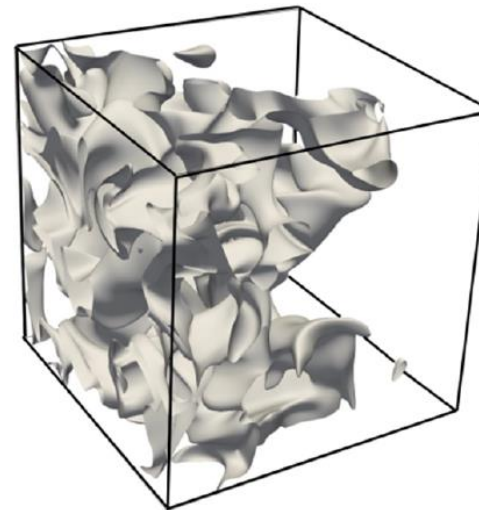
- Applications in Direct Injection (DI) engines and high altitude gas turbine relight
- Fundamental understanding is important for reducing NOx in engines and fire safety
- Reduces the possibility of misfires and improves ignition probability



MILD combustion



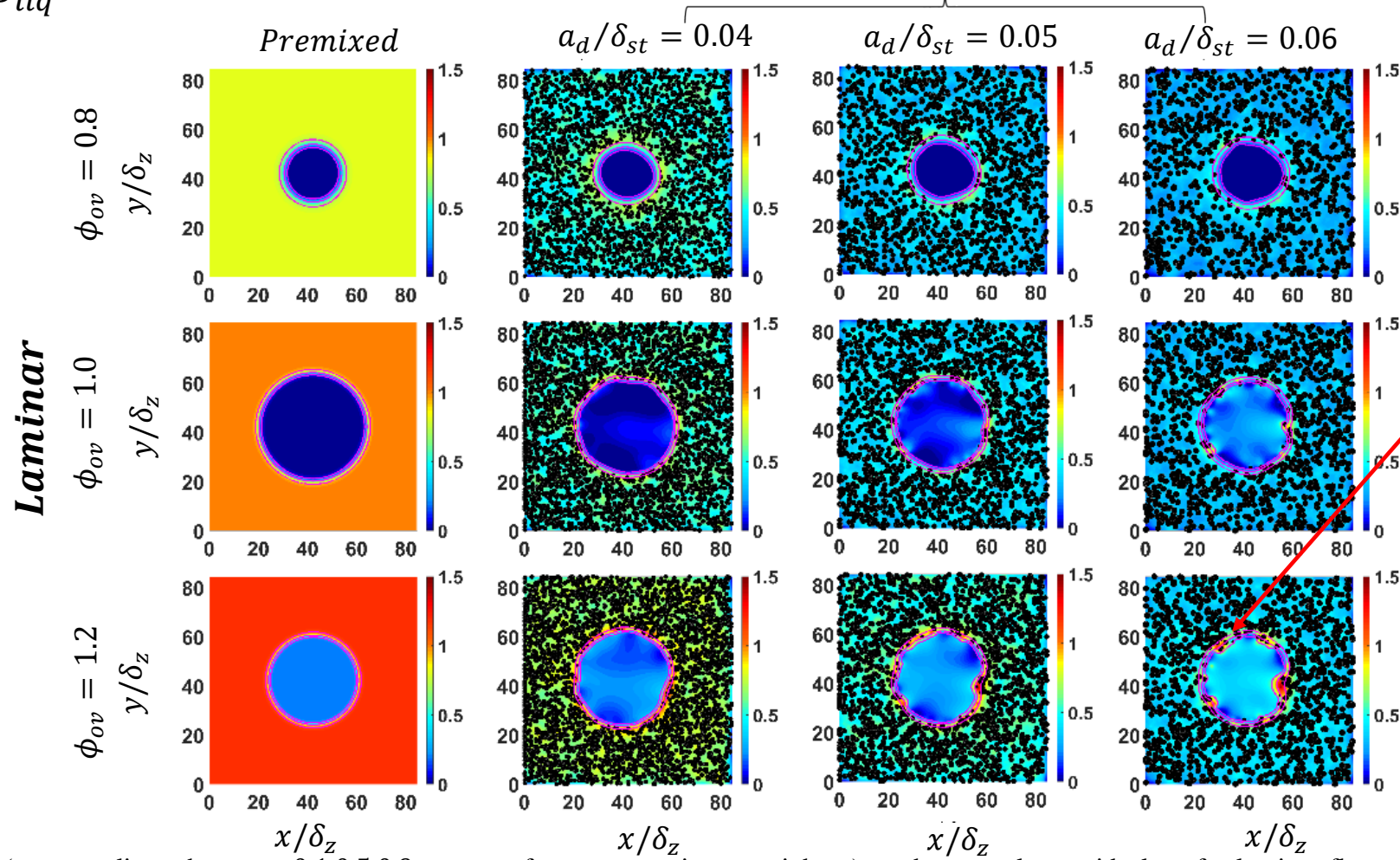
- Moderate or Intense Low oxygen Dilution (MILD) combustion can potentially improve thermal efficiency and reduce emissions.
- MILD combustion is realised when the initial mixture temperature T_0 is higher than the autoignition temperature T_{ign} and the maximum temperature rise due to combustion is smaller than the autoignition temperature $\Delta T < T_{ign}$.
- It is used in industrial furnaces and gas turbines for the advantages it offers in terms of NOx emission



Flame-droplet-turbulence interaction

$$\phi_{ov} = \phi_g + \phi_{liq}$$

$$u'/S_{b(\phi_g=1)} = 4.0$$

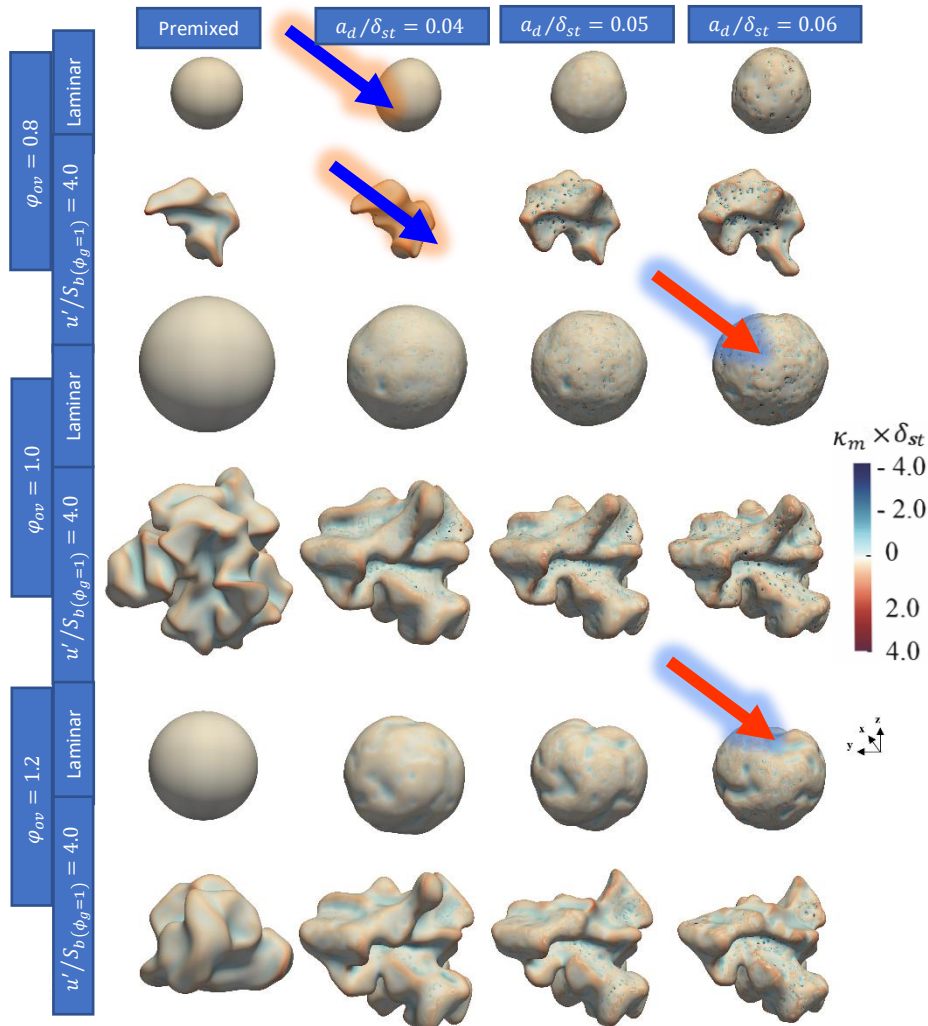


$$\phi = \frac{(F/A)}{(F/A)_{stoic}}$$

$\phi < 1$: Fuel – lean
 $\phi = 1$: Stoichiometric
 $\phi > 1$: Fuel – rich

Distribution of $Y_F/Y_{F,st}$ (magenta lines show $c = 0.1, 0.5, 0.9$ contours from outer to inner periphery) on the central x - y mid-plane for laminar flames with $\phi_{ov} = 0.8, 1.0$ and 1.2 . All figures correspond to $t = 2.52\alpha_{T0}/S_{b(\phi_g=1)}^2$

Droplet-induced flame wrinkling



$$\phi_{ov} = 0.8, 1.0, 1.2 \text{ and } a_d/\delta_{st} = 0.04, 0.05, 0.06$$

Flame normal vector:

$$\vec{N} = -\nabla c / |\nabla c|$$

Local curvature:

$$\kappa_m = \nabla \cdot \vec{N} / 2$$

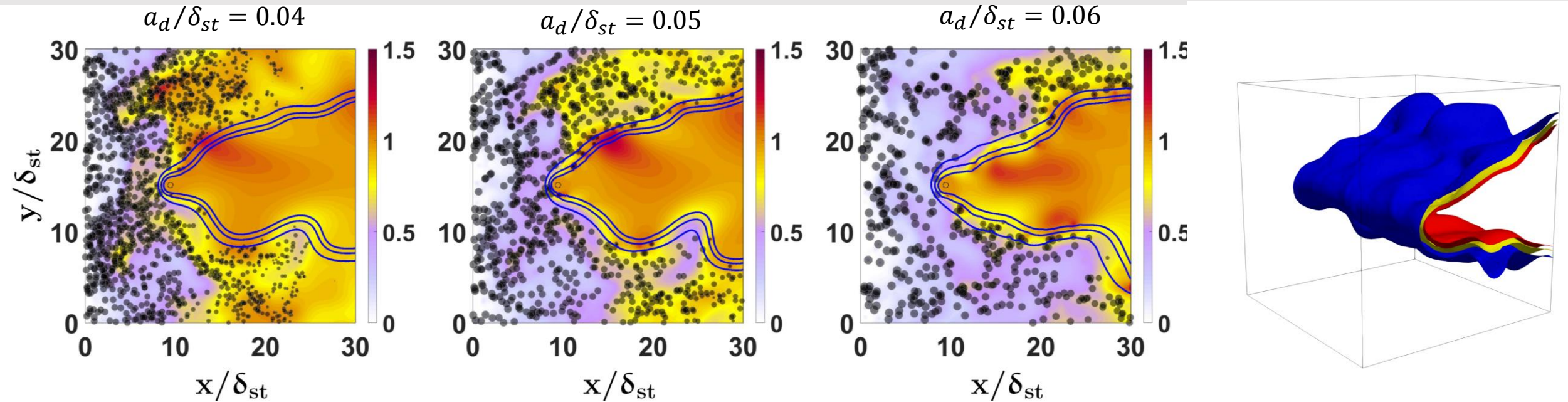
A positive curvature \rightarrow convex to the reactants

A negative curvature \rightarrow concave to the reactants

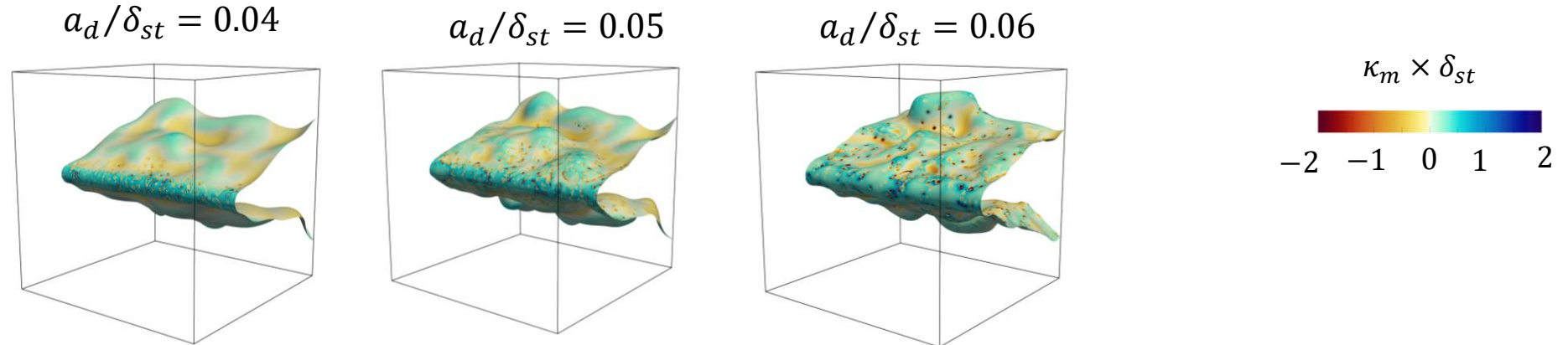
- ❖ The droplet case with initial $a_d/\delta_{st} = 0.04$ for $\phi_{ov} = 0.8$ does not show dimples but laminar flame also does not remain spherical.
- ❖ Evaporation of clustered droplets creates large distributed dimples for the $\phi_{ov} = 1.2$ cases in contrast to small densely packed dimples in the $\phi_{ov} = 1.0$ cases.

Instantaneous view of $c = 0.5$ isosurface coloured with local values of $\kappa_m \times \delta_{st}$ for the cases with $\phi_{ov} = 0.8$, $\phi_{ov} = 1.0$ and $\phi_{ov} = 1.2$ at $t = 2.52\alpha_{T0}/S_{b(\phi_g=1)}^2$.

Flame-droplet interaction for laboratory-scale configuration

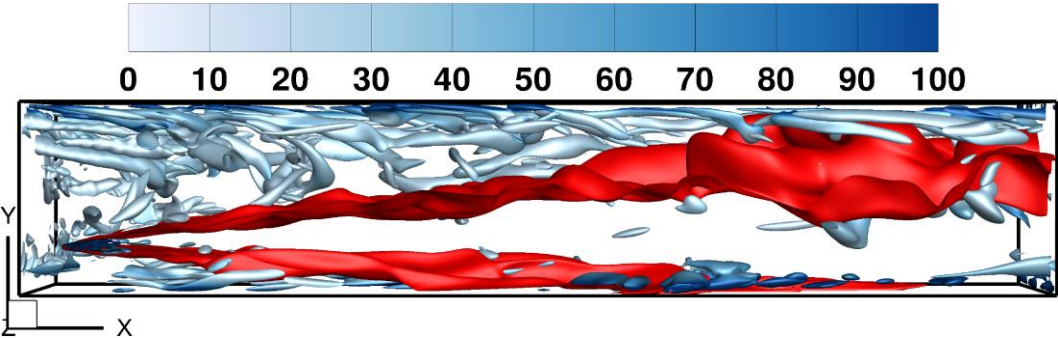


Instantaneous distributions of gaseous equivalence ratio, ϕ_g on the central x-y mid plane for statistically stationary rod-stabilised V-flames.

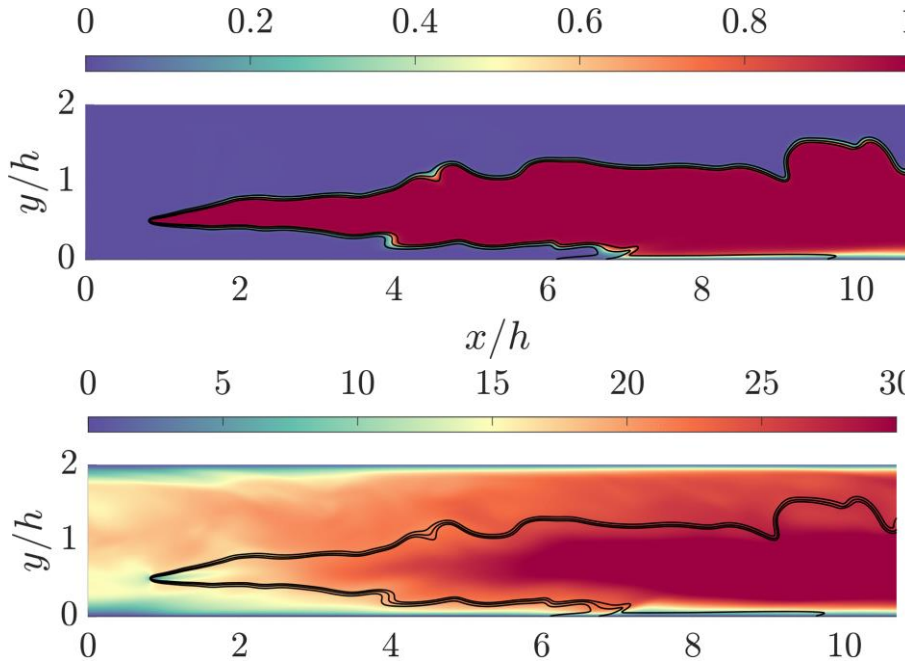


Simulation configurations in turbulent boundary layers

Oblique FWI for V-flames



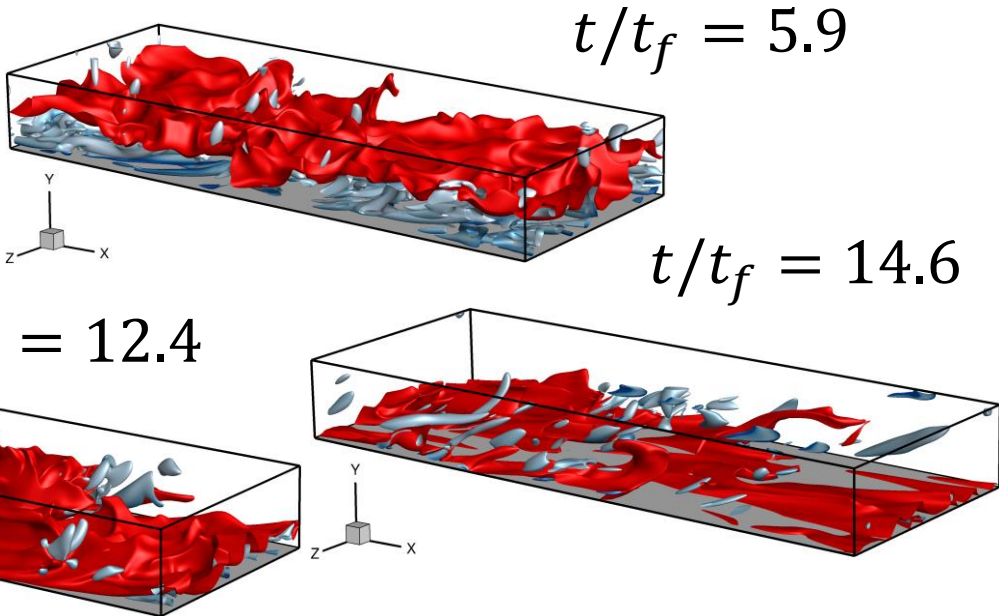
Q-criterion coloured by vorticity magnitude



Non-Dim. Temperature

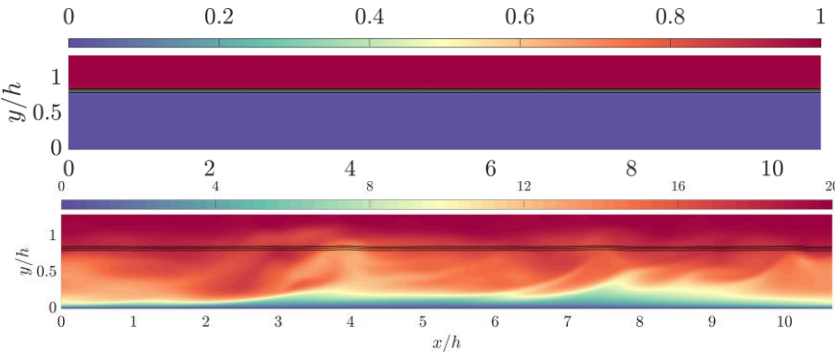
Non-Dim. Streamwise Velocity

Head-on interaction (HOI)

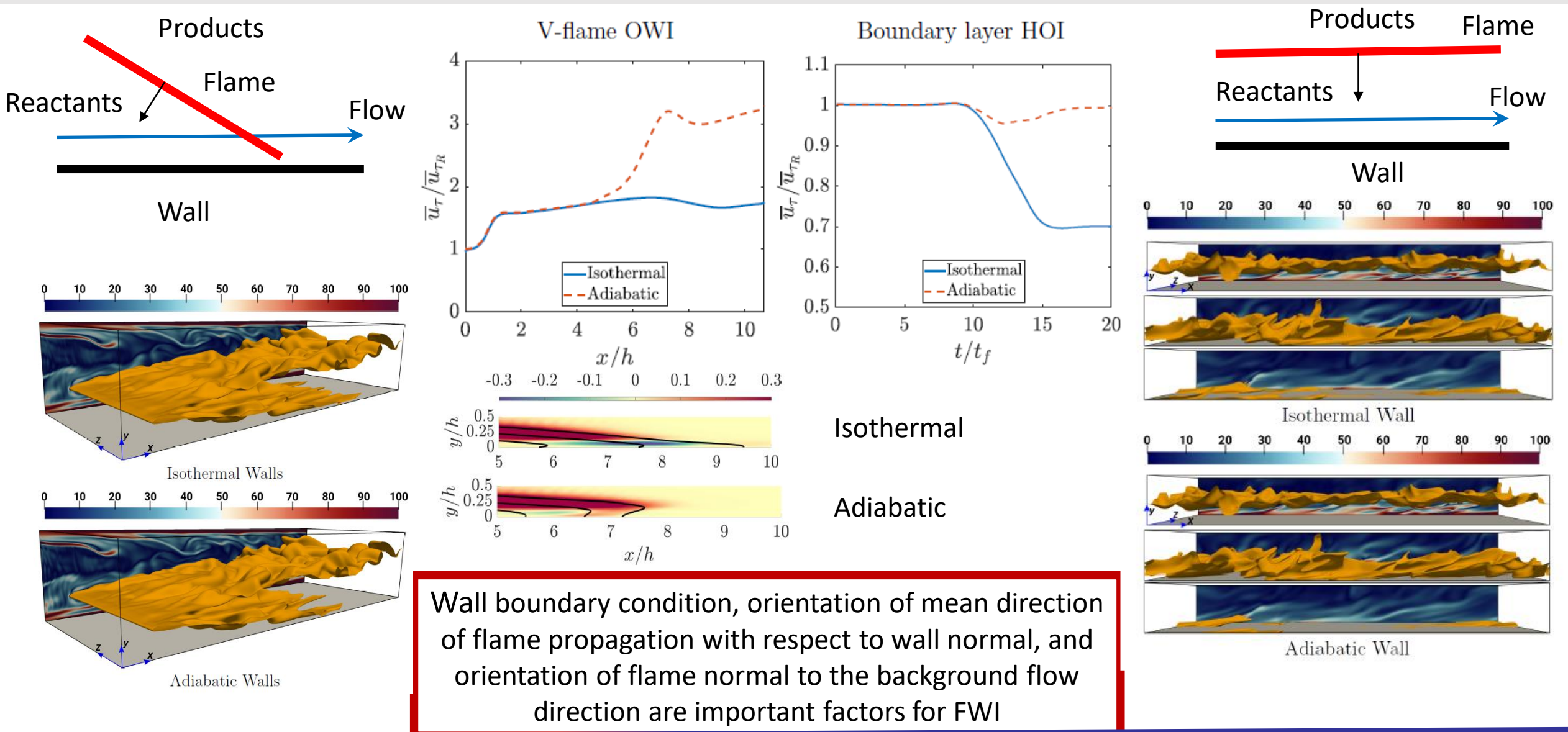


Q-criterion coloured by vorticity magnitude

Non-Dim. Temperature
Non-Dim. Streamwise Velocity



Mean shear stress at the wall for different boundary conditions



Importance of SENGGA+ Work Package

- 81% of the global energy demand is met by combustion but there is a need to move from the conventional fossil fuels to more environmentally friendly high hydrogen content (HHC) fuels (e.g. lean H_2 combustion, NH_3 combustion, NH_3 - H_2 blends and e-fuels) to tackle the problems of global warming and also for achieving net-zero targets.
- Hydrogen combustion chemistry is significantly different from hydrocarbon fuels and both atomic and molecular hydrogen induce significant amount of preferential diffusion. Thus, use of HHC fuels often bring challenges (e.g. flashback within turbulent boundary layers in gas turbines). Moreover, the existing combustion models may not perform well at high-pressure HHC fuel combustion where thermo-diffusive and hydrodynamic instabilities interact with each other.

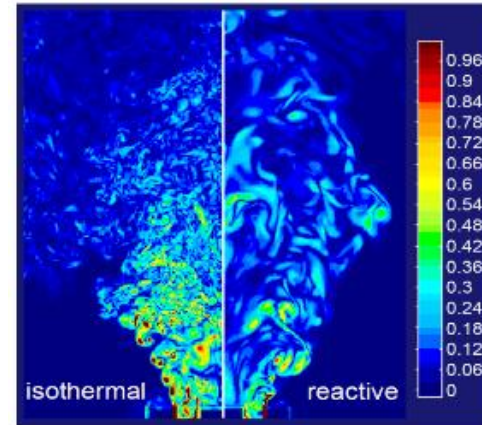


High-fidelity simulations enabled by SENGGA+ will help in terms of fundamental physical understanding which in turn will translate into model development for RANS and LES. RANS/LES equipped with accurate models will contribute to the development of next generation combustors.

Work Package & High-priority Use Cases

➤ Work Package of SENG+ will have following 4 sub work packages:

- (1) Re-Engineering of SENG+ with OPS
- (2) SENG+ high-level framework
- (3) Evaluation and validation of the new SENG+
- (4) High Priority Use Cases



(1) Premixed swirl flames for HHC fuels

(generic configuration for gas turbine combustors but challenging case for simulation and modelling for net-zero hydrogen based combustion)

(2) Turbulent boundary layer flashback for hydrogen-rich fuels

(important from the point of view of safety of operation and structural integrity in gas turbines for net-zero combustion of HHC fuels)

Thank you for your attention

